

Is Simultaneous Binding to DNA and Gyrase Important for the Antibacterial Activity of Cystobactamids?

Danny Solga⁺,^[a] Lianne H. E. Wieske⁺,^[b] Scott Wilcox⁺,^[b] Carsten Zeilinger,^[c] Linda Jansen-Olliges,^[c] Katarina Cirnski,^[d] Jennifer Herrmann,^[d] Rolf Müller,^[d] Mate Erdelyi,^{*[b]} and Andreas Kirschning^{*[a]}

Cystobactamids are aromatic oligoamides that exert their natural antibacterial properties by inhibition of bacterial gyrases. Such aromatic oligoamides were proposed to inhibit α -helix-mediated protein-protein interactions and may serve for specific recognition of DNA. Based on this suggestion, we designed new derivatives that have duplicated cystobactamid triarene units as model systems to decipher the specific binding mode of cystobactamids to double stranded DNA. Solution NMR analyses revealed that natural cystobactamids as well as their elongated analogues show an overall bent shape at their central aliphatic unit, with an average CX-CY-CZ angle of ~ 110

degrees. Our finding is corroborated by the target-bound structure of close analogues, as established by cryo-EM very recently. Cystobactamid CN-861-2 binds directly to the bacterial gyrase with an affinity of $9 \mu\text{M}$, and also exhibits DNA-binding properties with specificity for AT-rich DNA. Elongation/dimerization of the triarene subunit of native cystobactamids is demonstrated to lead to an increase in DNA binding affinity. This implies that cystobactamids' gyrase inhibitory activity necessitates not just interaction with the gyrase itself, but also with DNA via their triarene unit.

Introduction

Peptidic oligoamides are key elements in drug development. Medicinal chemists have expanded the structural space of basic peptide architectures by using monomeric building blocks other than α -amino acids, including those containing arenes and hetarenes (Figure 1).^[1] These architectures, represented by structures 1 and 2, can mimic secondary structures of proteins and nucleic acids. Depending on the choice of additional substituents (R^1 and R^2) on the aromatic ring, such foldamers are stabilized by intramolecular hydrogen bonds and exhibit

Protein and DNA binding of aryl and hetaryl oligoamides

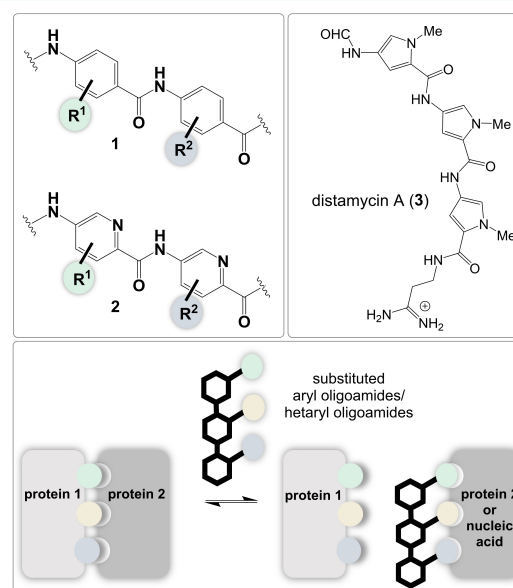


Figure 1. Top: *p*-Aminobenzoate (PABA) and pyridine-based oligoamide backbones 1 and 2 and natural hetaryl oligoamide distamycin A (3); bottom: aromatic oligoamides as potential inhibitors for α -helix mediated protein-protein or protein-nucleic acid interactions (R can be flexibly varied for finetuning properties of molecular recognition with the biological target) (the color code of the side chain is not linked to a specific functional group).

[a] Dr. D. Solga,⁺ Prof. Dr. A. Kirschning
Institute of Organic Chemistry, Leibniz University Hannover
Schneiderberg 1B, 30167 Hannover (Germany)
Fax: (+49) 511-762-3011
E-mail: andreas.kirschning@oci.uni-hannover.de

[b] Dr. L. H. E. Wieske,⁺ Dr. S. Wilcox,⁺ Prof. Dr. M. Erdelyi
Department of Chemistry - BMC, Uppsala University, Husargatan 3, SE-752
37 Uppsala, Sweden
E-mail: mate.erdelyi@kemi.uu.se

[c] Dr. C. Zeilinger, L. Jansen-Olliges
Institute of Biophysics and Center of Biomolecular Drug Research (BMWZ),
Leibniz University Hannover, Schneiderberg 38, 30167 Hannover, Germany

[d] Dr. K. Cirnski, Dr. J. Herrmann, Prof. Dr. R. Müller
Department of Microbial Natural Products, Helmholtz Institute for Pharma-
ceutical Research Saarland, Helmholtz Centre for Infection Research and
Saarland University, Campus E8.1, 66123 Saarbrücken, Germany

[⁺] These authors contributed equally to this work.

Supporting information for this article is available on the WWW under
<https://doi.org/10.1002/chem.202303796>

© 2024 The Authors. Chemistry - A European Journal published by Wiley-VCH GmbH. This is an open access article under the terms of the Creative Commons Attribution Non-Commercial NoDerivs License, which permits use and distribution in any medium, provided the original work is properly cited, the use is non-commercial and no modifications or adaptations are made.

folding modes that differ from those of peptidic foldamers, as depicted in Figure 2.^[2,3] Thus, sequence-specifically engineered synthetic aromatic oligoamides inhibit α -helix-mediated^[4] protein-protein interactions^[5,6] as was found in inhibiting the

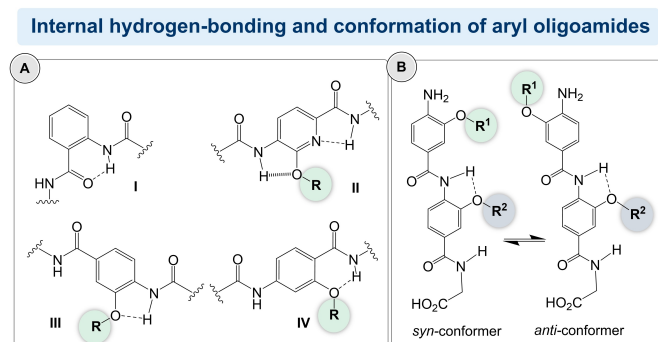


Figure 2. A) Various classes I–IV of oligoaromatic backbone monomers with key intramolecular hydrogen bonds, and B) possible *syn*–*anti*-conformers discussed in ref. [3c].

hDM2–p53 interaction,^[7] Bcl-x_L inhibitors^[8] and others^[8–12] (Figure 1).

Huc and coworkers developed a series of aromatic oligoamides that can mimic the DNA surface by forming α -helices. The anionic side chains on the outside of these single-stranded foldamers resemble those on the surface of B-DNA.^[13] However, pioneering work in this field was done by Dervan's group, who chose five-membered hetarenes, with the natural product distamycin A **3** serving as a lead structure for their studies. Pyrrole and imidazole rings, among others, served as structural insertions between an amino and a carboxyl group, and oligoarylamides derived from them could be developed that are specifically able to recognize DNA.^[14]

In essence, aromatic oligoamides behave like molecular chameleons in that they can conform to α -helices present in both proteins and DNA, and interfere with both protein–protein and protein–nucleic acid complexes. Nature has also come along this type of privileged structures^[15] in the form of the cystobactamids and albicidin but also distamycin A (**3**) and netropsin can be listed here.

Cystobactamids were first described by Müller and coworkers,^[16] who isolated them from myxobacteria of the genus *Cystobacter* sp. Cbv34. Later, they were also found in strains of the genera *Cystobacter*, *Myxococcus*, and *Coralloccoccus*. Cystobactamids **4–8**^[17] can be divided into two subclasses that carry either an iso- β -methoxyasparagine or a β -methoxy-asparagine moiety attached to the oligoarylamides (Figure 3).

Among the known naturally occurring cystobactamids, 861-2 (**8**) is the most active member inhibiting several clinically relevant Gram-positive and Gram-negative strains (*Acinetobacter baumannii*: MIC = 0.5 μ g/mL, *Citrobacter freundii*: MIC = 0.06 μ g/mL, fluoroquinolone-resistant *E. coli* WT-III *marRΔ74bp*: MIC = 0.5 μ g/mL, carbapenem-resistant *P. aeruginosa* CRE: MIC = 1.0 μ g/mL, and *Proteus vulgaris*: MIC = 0.25 μ g/mL)^[17] whereby the activity of bacterial type IIa topoisomerases is inhibited. Several total syntheses of cystobactamids^[17,18] have been reported as well as libraries of derivatives as part of a medicinal chemistry program.^[19]

Later, Kim and coworkers isolated cystobactamid derivatives from *Coralloccoccus coralloides*, which they named coralmycins A (**9**) and B.^[20] Finally, albicidin (**10**) is structurally closely related

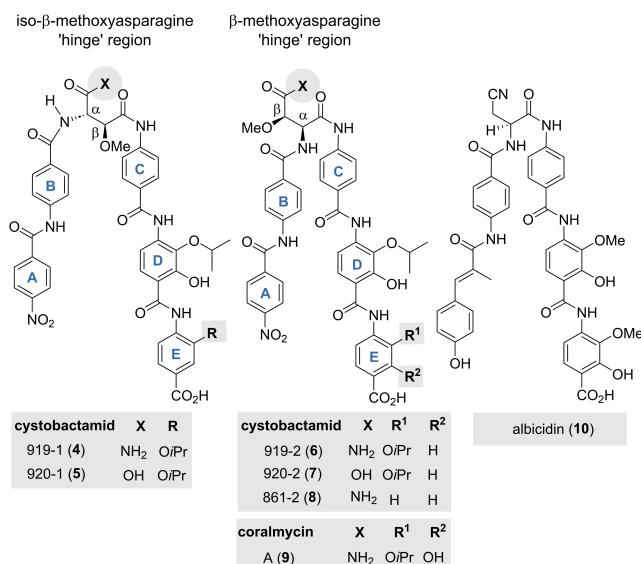


Figure 3. Structures of selected cystobactamids 919-1 (**4**), 920-1 (**5**), 919-2 (**6**), 920-2 (**7**), 861-2 (**8**), coralmycin (**9**) and of albicidin (**10**) (rings labelled A–E).

to the cystobactamids. First isolated in the 1980s from the phytopathogenic bacterium *Xanthomonas albilineans*, its structure elucidation took more than 30 years.^[21] Albicidin is highly similar to the cystobactamids and possess a nearly identical aromatic scaffold.

The exact mode of action of cystobactamids has been debated partly because bacterial type IIa topoisomerase works in combination with DNA. The first cryogenic electron microscopy (cryo-EM) structure of a ternary complex between *Escherichia coli* topoisomerase DNA gyrase, a 217bp double-stranded DNA fragment and albicidin (**10**) was determined very recently. The Süßmuth group demonstrated that albicidin obstructs the gyrase dimer interface and also intercalates between the fragments of the cleaved DNA. The findings suggest that DNA gyrase is inhibited from religating DNA.^[22]

It is well known that helically mediated binding properties of (het)aromatic oligoamides can be enhanced by elongation.^[15] These findings combined with the results on albicidin^[22] encouraged us to prepare extended cystobactamids (Figure 4). Herein they are used to explore the importance of binding to the protein or dsDNA or both for exerting the antibacterial activity of the cystobactamids.

The structural studies on albicidin indicate that the coumaric acid unit linked to one PABA unit interacts with double stranded DNA (dsDNA), while the three amide-linked aromatic rings interact with gyrase. Thus, the latter moiety is duplicated in the new cystobactamid derivatives **12a–c** and **13a** and **13b** to directly affect or even suppress the interaction with the protein. If the biological effect was maintained, this would allow conclusions to be drawn about the importance of the interaction of the coumaric acid unit linked to one PABA unit (resembling A and B rings of the cystobactamids, Figure 3) for the antibacterial activity. Thus, this study is not about the preparation of more active cystobactamids, knowing that

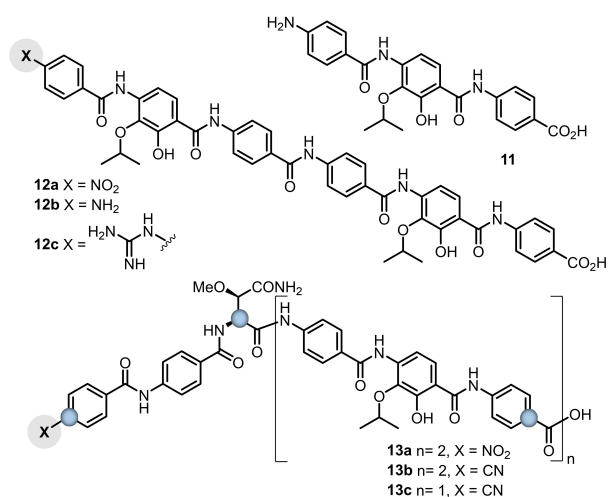


Figure 4. Structures of oligo-*p*-aminobenzoates **11** and **12a–c** and extended cystobactamids **13a** and **13b** and cyano derivative of cystobactamid CN-861-2 (**13c**), which are synthetic targets of the present work. Atoms highlighted in blue are used for superpositioning of the 3D-conformations and determination of the angle for the bent shape of the respective compounds and are further indicated as CX-CY-CZ (see figures 5 and 6).

eventually the membrane permeability may be reduced by the extension, but wishes to shed light on the role of the cystobactamid subunits on binding that is associated with biological activity.

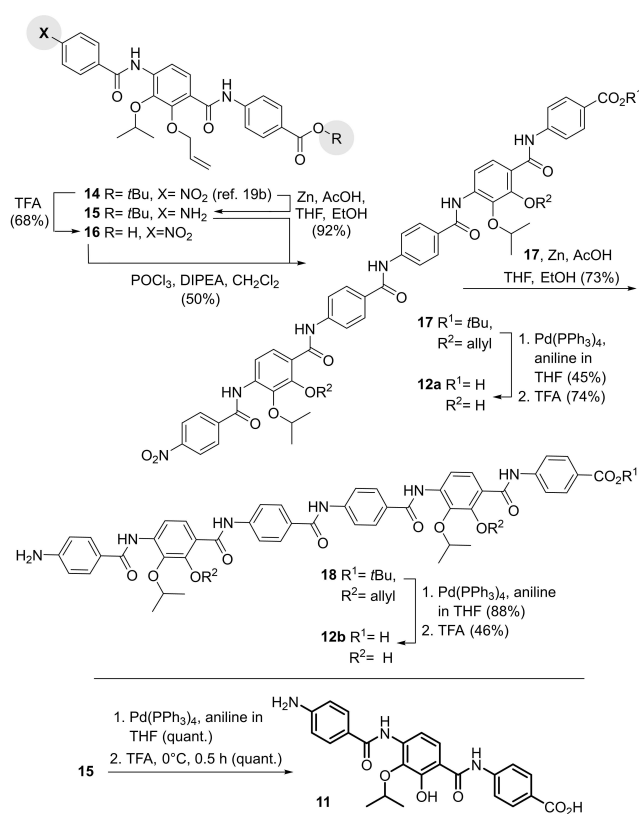
Results and Discussion

Synthesis: Starting from the known synthetic oligo-*p*-aminobenzoates and their structural similarities to cystobactamids, we dimerized the triaryl Et_3N (rings C–E), added different functional groups at the amino terminus, and prepared the corresponding extended cystobactamids in which the nitro group was replaced by the cyano group.

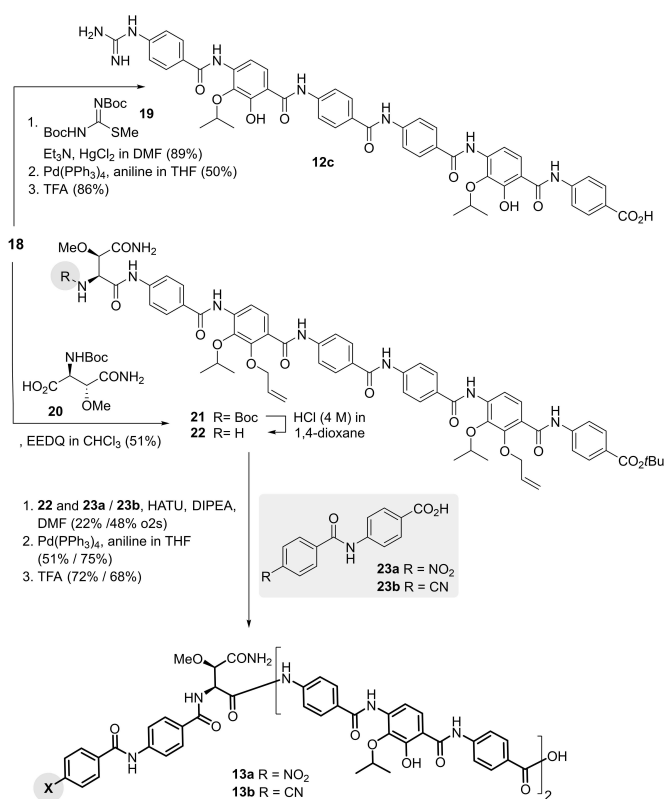
These were designed to a) provide insight into the preferred conformations of cystobactamids and b) serve as tools to study the ability of cystobactamids to bind to DNA.

The modular synthesis commenced from known oligoamide **14**.^[19b] Both terminal functionalities, the nitro and the *t*Bu ester groups, were successively converted to either an amino or a free carboxylic acid to form building blocks **15** and **16**, respectively (Scheme 1). Both triarenes were coupled after activation of the carboxylate as an acyl chloride to give the pentaamide **17**, which after deprotection gave the linear pentaamide **12a**. The nitro group in hexarene **17** served as a starting point for further functional group manipulations by reduction to the amine **18**, followed by hydrolysis to **12b** and then converting it to guanidino **12c** with reagent **19** (Scheme 2).

Alternatively, the free amino group in pentaamide **18** was coupled with the methoxyasparagine building block **20**, prepared according to the earlier published protocol.^[19b] Amide coupling was promoted by EEDQ and after removal of the Boc group intermediate **22** was obtained. From here, the amides



Scheme 1. Synthesis of dimers **12a** and **12b** and triarene **11**.



Scheme 2. Synthesis of dimer **12c** and elongated cystobactamid derivatives **13a** and **13b**.

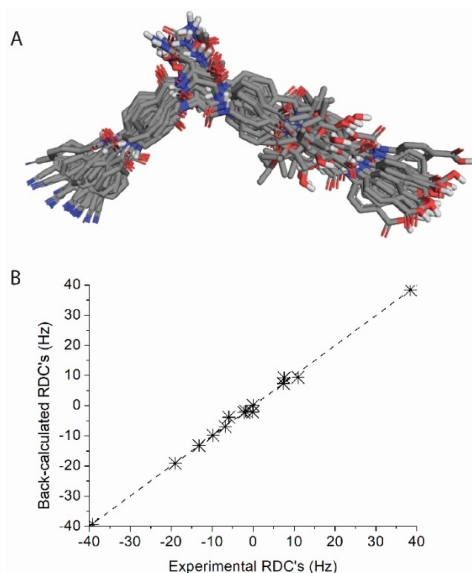


Figure 5. (A) Superposition of the 21 conformations of **13c** as selected by the analysis of RDC's, and (B) the correlation between the experimental and back-calculated RDC's ($R^2 = 0.99$).

23a and **23b**, the former bearing the nitro group of natural cystobactamids, the latter modified by the nitrile group providing cystobactamids with improved antibacterial properties,^[19b] were linked to the free amino group of the methoxyasparagine moiety. After Pd-mediated removal of the allyl protecting group and ester hydrolysis, the two new elongated cystobactamids **13a** and **13b** with the dimeric pentaamide chain were obtained.

Conformational analysis: To determine the solution structure of **13c**, we carried out conformational analyses using two independent methods, Nuclear Overhauser effect (NOE) and Residual dipolar coupling (RDC)-analyses, cross-validating their outcome against each other. The ^1H and ^{13}C NMR-assignments for **13b**, the fragment **12b** and the cystobactamid CN-861-2 (**13c**) in $\text{DMSO-}d_6$ were based on ^1H , ^{13}C , HSQC, HMBC and NOESY spectra. The first conformational information came from extensive NOESY analyses for **13b** and **13c**. Due to signal overlap (Tables S5–S6, SI), the NOE-analyses of **13b** and **13c** resulted in two sets of semi-quantitative interproton distances.^[26] A total of 51 relevant NOE's were observed for

13b, and 47 for **13c** which were divided into long- and short-range correlations. The proton-pairs most likely giving rise to each observed NOE were identified, for both compounds, by a thorough manual comparison of the experimentally obtained distances to the interproton distances present in the theoretical ensembles (generated by unrestrained Monte Carlo systematic torsional sampling) (Tables S7–S8, SI).

Through this process, by focussing on the most informative long-range NOE's, we identified ensembles consisting of 49 conformations for **13b**, and of 33 conformations for **13c** in line with the obtained NOE correlations. These conformers are most compatible with long-range NOE's; however, we cannot exclude the presence of additional conformers for which the NOE is above 5 Å with a non-negligible population. Importantly, the common moieties of **13b** and **13c** have a large number of analogous NOE's of comparable relative cross-peak intensities, which suggest that they adopt a similar bent 3D structure in solution (SI, pages S17–S19).

The solution conformation of cystobactamid CN-861-2 (**13c**) was further studied based on the 14 $^1D_{\text{C,H}}$ residual dipolar couplings (RDC's) that were found. These RDC's were well-distributed along the entire length of the molecule (Table S11, SI).^[27,28] We used the software MSpin^[29] to identify the solution ensemble, based on singular value decomposition (SVD) analysis of the RDC's. This provided a solution ensemble consisting of 21 conformers, each having a low molar fraction, which is expected for a comparably flexible molecular system (Figure 5A, and Table S12, SI). The experimental and the population-weighted, back-calculated RDC's of the ensemble show an excellent fit (Figure 5B), with the viability of the analysis being confirmed by the Q-factor of 0.06 (acceptable < 0.3) and the SVD number of 6.6 (acceptable < 30).^[30] The conformational ensembles that were identified in the NOE-analyses of **13b** and **13c**, and that identified by RDC analysis are highly similar. The conclusions of the three analyses coincide in **13b** and in cyano cystobactamid CN-861-2 (**13c**) showing an overall bent shape at the central aliphatic unit, with an average CX-CY-CZ angle of ~ 110 degrees (Figure 6 and Table 1, populations are given in Table S12, SI).

The aromatic oligoamide units in contrast are extended and linear, stabilized by intramolecular hydrogen bonds that is reflected by the large chemical shift of the amide protons ($\delta \sim 9\text{--}12$ ppm, Table S4, SI). The cystobactamid **13c** was found to

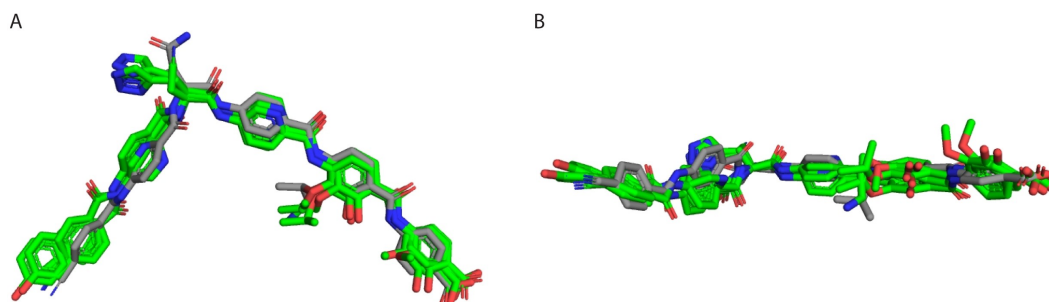


Figure 6. The superposition of the structures of the target-bound structure of four albicidin analogues, as identified by cryo-EM, in green, and of a selected RDC solution conformation of **13c** (black) indicate vast similarities. Subfigures **A** and **B** differ by a 90 degrees rotation.

Table 1. Minimum, average and maximum angle found between the highlighted carbon atoms in figure 4 of the conformations based on NOESY data for **13b** and **13c**, and as determined from the solution ensemble for **13c** obtained by RDC analysis.

	13b	13c	RDC
	NOESY	NOESY	
Minimum angle (degrees)	77	87	87
Average angle (degrees)	109	113	108
Maximum angle (degrees)	146	148	147

prefer a dynamic yet overall bent structure in solution. This solution ensemble is expected to contain the bioactive conformation that is necessary for DNA binding, as a major conformational adjustment upon binding would require more energy than that available at physiological temperature. Furthermore, the target-bound structure of flexible bioactive compounds have been found to be present in solution. We also found that the target-bound conformations exist in both polar and apolar environments. It is therefore likely that the bioactive conformation is present in the obtained solution ensembles.

In view of the four cryo-EM data of the *E. coli* topoisomerase DNA gyrase complexed with albicidin analogues collected by Süssmuth and Ghilarov^[22] we found that the solution structures for **13c** identified by RDC analysis display a remarkably similar fold to those reported for albicidin (**10**) by cryo-EM. The aromatic rings of the latter show a twisting orientation with respect to each-other, each showing a slight offset from the previous aromatic unit. Conformations showing similar twisting orientation were also identified in the ensemble of cystobactamid CN-861-2 (**13c**) by RDC analysis. The CX-CY-CZ angles of the four albicidin analogues, 90–95 degrees, fall within the ranges observed for **13b,c** by NOESY and RDC-based analyses (77–148 degrees, Table 1).

Biological activity: Finally, the *in vivo* activity of the extended cystobactamids was tested. The results are summarized in Tables 2 and 3, and S2. The MIC data show that fragment **11** as well as cystobactamids **12a-c** (potentially only binding DNA) do not exhibit antibacterial activity but result in considerably reduced biological activity. Considering also the studies on albicidin, it is apparent that the DNA-binding “eastern part” is essential for the antibacterial activity. Duplication of the C–E rings does not necessarily result in complete

Table 3. Cytotoxicity of **11**, **12a**, **12b**, **12c**, **13a** and **13b** against a panel of cell lines. Given are IC₅₀ values in µg/ml.

cell line	11	12a	12b	12c	13a	13b
HCT-116	>37	>37	>37	>37	>37	>37
U-2 OS	>37	27.4	14.2	>37	>37	>37
CHO-K1	>37	>37	>37	>37	>37	>37

loss of antibacterial activity, as revealed by comparison of the extended derivative **13b** with the known cystobactamid CN-861-2 (**13c**), where we found depending on the strain only 4- to 32-fold reduced potency for the extended derivative **13b**.

The reduced activity of **13a** as compared to that of **13b**, i.e., upon the replacement of the nitro group by the cyano group, is not unexpected, as this is similarly true for the truncated representatives. In addition, the enlarged size of the expanded cystobactamids may hinder transmembrane uptake into the bacterial cell. None of the cystobactamids tested exerted antifungal activity. Interestingly, an unusual growth pattern was observed in *C. neoformans* and *P. anomala* when exposed to compounds **12c**, **13a**, and **13b**. In addition, cytotoxicity testing using three different cancer cell lines did not reveal any pronounced biological activity of the tested cystobactamids. However, we observed inhibitory activity of the extended cystobactamids **12a** and **12b** against human U-2 OS osteosarcoma cells with IC₅₀ of 27.4 and 14.2 µg/mL, respectively.

However, the structural data recently obtained by Ghilarov by cryo-EM^[22] still leave one aspect unanswered and that is the direct relationship between the gyrase and the dsDNA.

As this assay may not be sensitive enough, we have clarified this point in more detail, by developing a thermophoresis assay to determine whether CN-861-2 **13c** can bind directly to the gyrase of *E. coli*. Figure 7A shows the binding kinetics of **13c** at various concentrations, from which a binding constant (K_d) of 9 µM ± 3 µM could be determined (Figure 7B), with complete inhibition observed at 50 µM. Indeed, this result indicates that cystobactamid CN-861-2 **13c** interacts directly with DNA gyrase. This correlates well with the determined relaxation kinetics for albicidin^[22] for which complete inhibition of topo-IV relaxation activity was determined at 100 µM.

Table 2. Antibacterial activity of **11**, **12a**, **12b**, **12c**, **13a** and **13b** against a panel of Gram-negative and Gram-positive bacteria compared to CN-861-2 (**13c**). Given are MIC values in µg/ml (an extension of data are found in table S1 in the supporting information).

strain	11	12a	12b	12c	13a	13b	13c
<i>A. baumannii</i> DSM-30008	>64	>64	>64	>64	>64	64	2
<i>C. freundii</i> DSM-30039	>64	>64	>64	>64	64	8	0.25
<i>E. coli</i> BW25113 (WT)	>64	>64	>64	>64	16	1	0.125
<i>E. coli</i> JW0451-2 (ΔacrB)	>64	>64	>64	>64	16-64	0.25	≤0.03
<i>P. vulgaris</i> DSM-2140	>64	>64	>64	>64	64	8	2
<i>B. subtilis</i> DSM-10	>64	>64	>64	>64	16	2	0.25
<i>S. aureus</i> Newman	>64	>64	>64	>64	16	2	0.125

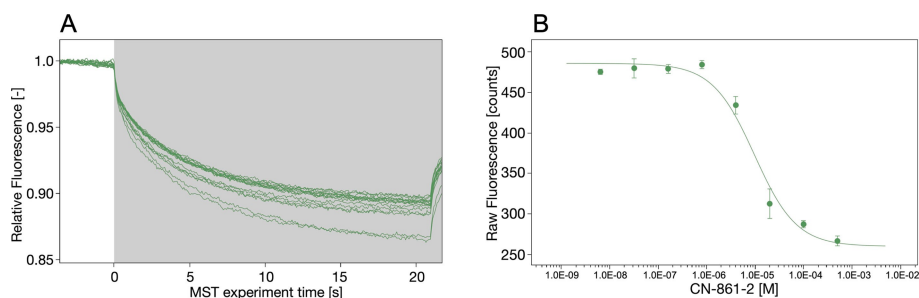


Figure 7. Evaluation of the binding affinity of CN-861-2 **13c** for *E. coli* gyrase. **A.** Relative fluorescence of FITC labeled *E. coli* gyrase as a function of time at different concentrations of CN-861-2 from 500 μM to 6.4 nM. The color of blue and red represent F_{cold} and F_{hot} respectively, which show the positions of data collection. **B.** Affinity binding curve of CN-861-2. The FITC-gyrase concentration was kept constant at 50 nM. The ΔF data were normalized and fitted in the K_d model.

In addition, we determined the binding of CN-861-2 **13c** to DNA by a thermophoresis assay, using a primer that was used in reference 22 and that is shorter than the 217 bp DNA fragment. For this purpose, we used single-stranded Cy5-labeled DNA (50 nM) and the unlabeled complementary strand. We analyzed pairs with high AT or alternatively high GC content. No binding was detected under these conditions (Figure S1).

We supplemented this study with a second method that allows determination of the DNA affinity of CN-861-2 **13c**. We used an AT-rich dsDNA sequence (1 μM) for a fluorescence competition assay in the presence of 1 μM of the DNA binding agent SYBR Green I. The concentrations of triarylamide **12**, cystobactamids CN-861-2 **14c**, **13a–c**, and **14a–b** were varied to quantify DNA binding affinity and to investigate the displacement of the minor groove binder SYBR Green I. The titration curves (Figure 8) show the displacement of SYBR Green I in the presence of each of the oligoamides tested.

In general, the concentrations required for 50% displacement (EC_{50}) of SYBR Green I decrease with increasing cystobactamid length. The EC_{50} values show that the elongated cystobactamids (**13a**, **14a** and **14b**) have a higher binding affinity towards dsDNA than the shorter ones. This suggests that the derivative CN-861-2 **13c** also binds to DNA. In addition, the change in anisotropy as a function of AT- and GC-DNA concentration was examined. Again, binding via AT-rich DNA is

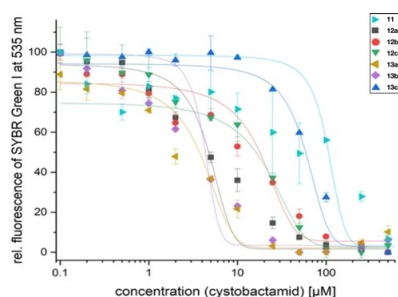


Figure 8. Displacement titration of SYBR Green I bound to AT-rich dsDNA as a function of cystobactamid concentration. The relative fluorescence of SYBR Green I bound to dsDNA at 535 nm is shown as a function of the concentration of cystobactamid. The graphs were fitted using Dose-Response function.

preferred at low DNA concentrations (Figure S2). This led to the consideration that if the primer DNA is occupied by CN-861-2 **13c**, it should also be unavailable in the PCR reaction. Indeed, this can be shown for several cystobactamid derivatives (Figure S3).

Even if our thermophoresis experiments show that CN-861-2 **13c** binds directly to labeled gyrase,^[30] we cannot exclude that CN-861-2 and its derivatives favorably bind to the corresponding AT-rich DNA regions and these segments may then be integrated into the gyrase as novel DNA intercalators. Further structural studies are required to underpin this finding.

Conclusions

We report the total synthesis of a series of novel cystobactamids, whose specific structural feature is the duplication of their cystobactamid triarene unit. Solution NMR studies using two independent methods, NOE and RDC analyses, demonstrate that the conformation of cystobactamids in solution closely resembles the protein-bound structure that was recently found using cryo-EM. The solution ensembles found contain conformations around their central α -amino acid with angles ranging from 80 to 150 degrees and an average of $\sim 110^\circ$ thereby covering the 90 degrees found for the bioactive conformation. Thus only minor conformational adjustments are necessary for binding to their biological target.

Thermophoresis experiments reveal that gyrase binds cystobactamid CN-861-2 **13c** and that the extended derivatives **13a,b** show improved binding to DNA compared to the shorter cystobactamids. Although the DNA binding of the cystobactamids with the triarene repeat is more pronounced than with CN-861-2 **13c** this is in no way reflected in the bioactivity data. This observation is likely associated with differences in uptake which directly is linked to bioactivity. Thus membrane permeability is supposedly lower for the extended derivative **13b** due to the greater molecular size.

It is particularly important to highlight that the synthetically elongated cystobactamid derivatives show a preference for binding to AT-rich over GC-rich dsDNA. Our data demonstrate that simultaneous binding to both the dsDNA and the gyrase is

essential for the antibacterial activity of cystobactamid, whereas binding to the protein alone is insufficient.

Experimental Section

The experimental section below covers synthetic key protocols for preparing cystobactamids, lists of analytic and spectroscopic data and protocols to evaluate their biological properties. General experimental information as well as copies of NMR spectra are found in the supporting information. Original NMR data (FIDs), assignment (NMReDATA), details of the RDC-based conformational analyses, and the solution conformations (mol2) are available free of charge on the open repository Zenodo with DOI:10.5281/zenodo.7038646.

Chemical Syntheses

Triarene 11

Tetrakis(triphenylphosphine)palladium(0) (21 mg, 18 μ mol, 0.10 eq.) was added in one portion to a stirred solution of allyl ether **15**^[19b] (100 mg, 183 μ mol, 1.00 eq.) and aniline (0.06 mL, 605 μ mol, 3.30 eq.) in THF (8.0 mL). After stirring overnight, the mixture was concentrated in the presence of silica gel *in vacuo*. Flash column chromatography (PE/EtOAc = 1/1, 1/2) furnished phenol **S1** (93 mg, 183 μ mol, >99%) as a yellow foam.

¹H-NMR (500 MHz, DMSO-*d*₆): δ = 12.37 (s, 1 H, OH), 10.58 (bs, 1 H, CONH-7), 8.98 (s, 1 H, CONH-12), 7.93–7.91 (m, 2 H, H-10, H-10'), 7.86–7.81 (m, 4 H, H-5, H-6, H-9, H-9'), 7.67–7.65 (m, 2 H, H-14, H-14'), 6.65–6.63 (m, 2 H, H-15, H-15'), 5.92 (bs, 2 H, NH₂), 4.59 (septet, *J* = 6.2 Hz, 1 H, CHMe₂), 1.55 (s, 9 H, CO₂CMe₃), 1.28 (d, *J* = 6.1 Hz, 6 H, CHMe₂) ppm; ¹³C-NMR (125 MHz, DMSO-*d*₆): δ = 168.7 (q, C-7), 164.6 (q, CO₂CMe₃), 164.4 (q, C-12), 154.1 (q, C-3), 152.8 (q, C-16), 142.0 (q, C-8), 137.7 (q, C-1), 135.0 (q, C-2), 129.9 (t, C-10, C-10'), 129.0 (t, C-14, C-14'), 126.8 (q, C-11), 122.9 (t, C-5), 120.7 (t, C-9, C-9'), 119.9 (q, C-13), 113.0 (t, C-15, C-15'), 111.3 (q, C-4), 110.8 (t, C-6), 80.5 (q, CO₂CMe₃), 74.7 (t, CHMe₂), 27.9 (p, CO₂CMe₃), 22.4 (p, CHMe₂) ppm; HRMS (ESI): *m/z* calculated for C₂₈H₃₁N₃O₆Na [M + Na]⁺: 528.2111; found: 528.2109; R_f (PE/EtOAc = 1/1): 0.41.

Ester **S1** (93 mg, 183 μ mol, 1.00 eq.) was dissolved in trifluoroacetic acid (10.2 mL) at 0 °C. After stirring at room temperature for 30 min, the mixture was cooled to 0 °C. Then, Et₂O (100 mL) was poured into the reaction mixture. The resulting precipitate was filtered, washed with an excess of Et₂O, and dried *in vacuo* to furnish triarene **11** (83 mg, 183 μ mol, >99%) as a yellow foam.

The analytical data are in accordance with those reported in the literature.^[19a]

¹H-NMR (500 MHz, DMSO-*d*₆): δ = 12.80 (bs, 1 H, CO₂H), 12.37 (s, 1 H, OH), 10.57 (s, 1 H, CONH-7), 9.00 (s, 1 H, CONH-12), 7.97–7.96 (m, 2 H, H-10, H-10'), 7.86–7.81 (m, 4 H, H-5, H-6, H-9, H-9'), 7.68–7.66 (m, 2 H, H-14, H-14'), 6.67–6.65 (m, 2 H, H-15, H-15'), 4.58 (septet, *J* = 6.1 Hz, 1 H, CHMe₂), 1.28 (d, *J* = 6.2 Hz, 6 H, CHMe₂) ppm; ¹³C-NMR (125 MHz, DMSO-*d*₆): δ = 168.7 (q, C-7), 166.9 (q, CO₂H), 164.4 (q, C-12), 154.1 (q, C-3), 152.4 (q, C-16), 142.0 (q, C-8), 137.7 (q, C-1), 135.0 (q, C-2), 130.2 (t, C-10, C-10'), 129.0 (t, C-14, C-14'), 126.3 (q, C-11), 122.9 (t, C-5), 120.8 (t, C-9, C-9'), 120.2 (q, C-13), 113.2 (t, C-15, C-15'), 111.3 (q, C-4), 110.9 (t, C-6), 74.7 (t, CHMe₂), 22.4 (p, CHMe₂) ppm; HRMS (ESI): *m/z* calculated for C₂₄H₂₂N₃O₆ [M-H]⁻: 448.1509; found: 448.1512. R_f (PE/EtOAc = 1/1): 0.21.

Triarene 16

Precooled TFA (69 mL) was slowly added to ester **14** (1.00 g, 1.74 mmol, 1.00 eq.) at 0 °C. Subsequently, the reaction mixture was allowed to warm to room temperature over 30 min. Then, Et₂O (120 mL) was poured into the mixture at 0 °C. The resulting precipitate was filtered (washing with an excess of Et₂O) and dried *in vacuo* to furnish carboxylic acid **16** (702 mg, 1.35 mmol, 78%) as a pale yellow foam.

¹H-NMR (400 MHz, DMSO-*d*₆): δ = 12.75 (bs, 1 H, CO₂H), 10.56 (s, 1 H, CONH-7), 10.15 (s, 1 H, CONH-15), 8.39 (d, *J* = 8.8 Hz, 2 H, H-18, H-18'), 8.22 (d, *J* = 8.8 Hz, 2 H, H-17, H-17'), 7.94 (d, *J* = 8.7 Hz, 2 H, H-13, H-13'), 7.83 (d, *J* = 8.7 Hz, 2 H, H-12, H-12'), 7.68 (d, *J* = 8.4 Hz, 1 H, H-6), 7.41 (d, *J* = 8.4 Hz, 1 H, H-5), 6.02 (ddt, *J* = 17.1, 10.9, 5.4 Hz, 1 H, H-9), 5.37 (pseudo dq, *J* = 17.2, 1.6 Hz, 1 H, H-10 *trans*), 5.20 (pseudo dq, *J* = 10.4, 1.3 Hz, 1 H, H-10 *cis*), 4.62 (d, *J* = 5.5 Hz, 2 H, H-8), 4.48 (septet, *J* = 6.1 Hz, 1 H, CHMe₂), 1.24 (d, *J* = 6.1 Hz, 6 H, CHMe₂) ppm; ¹³C-NMR (100 MHz, DMSO-*d*₆): δ = 166.9 (q, CO₂H), 164.6 (q, C-7), 163.8 (q, C-15), 149.7 (q, C-3), 149.3 (q, C-19), 143.8 (q, C-2), 143.0 (q, C-11), 139.8 (q, C-16), 134.9 (q, C-1), 133.7 (t, C-9), 130.4 (t, C-13, C-13'), 129.1 (t, C-17, C-17'), 128.4 (q, C-4), 125.5 (q, C-14), 123.8 (t, C-18, C-18'), 123.4 (t, C-5), 120.4 (t, C-6), 118.9 (t, C-12, C-12'), 117.8 (s, C-10), 76.3 (t, CHMe₂), 74.3 (s, C-8), 22.3 (p, CHMe₂) ppm; HRMS (ESI): *m/z* calculated for C₂₇H₂₅N₃O₆Na [M + Na]⁺: 542.1539; found: 542.1544; R_f (PE/EtOAc = 1/1): 0.19.

Hexaarene 17

A solution of carboxylic acid **16** (600 mg, 1.15 mmol, 1.00 eq.) and amine **15** (599 mg, 1.10 mmol, 0.95 eq.) dissolved in CH₂Cl₂ (3.8 mL) was cooled to 0 °C. Then, DIPEA (0.34 mL, 1.96 mmol, 1.70 eq.) and POCl₃ (0.11 mL, 1.15 mmol, 1.00 eq.) were added dropwise and the reaction mixture was stirred for 24 h while slowly warming up to room temperature. Subsequently, sat. aq. NH₄Cl was added, the phases were separated, and the aqueous phase was extracted with CH₂Cl₂ (3x 20 mL). The combined organic phases were dried over MgSO₄, filtered, and concentrated in the presence of silica gel *in vacuo*. Flash column chromatography (PE/EtOAc = 4/1 – 2/1 – 1/1) afforded amide **17** (578 mg, 0.55 mmol, 50%) as a colorless foam.

¹H-NMR (400 MHz, DMSO-*d*₆): δ = 10.56 (s, 1 H, CONH), 10.53 (s, 1 H, CONH), 10.46 (s, 1 H, CONH), 10.16 (s, 1 H, CONH), 9.56 (s, 1 H, CONH), 8.40 (d, *J* = 8.8 Hz, 2 H, Ar-H), 8.22 (d, *J* = 8.8 Hz, 2 H, Ar-H), 8.04–7.97 (m, 6 H, Ar-H), 7.92–7.83 (m, 7 H, Ar-H), 7.71 (d, *J* = 8.4 Hz, 1 H, Ar-H), 7.45–7.41 (m, 2 H, Ar-H), 6.09–5.98 (m, 2 H, =CH–), 5.42–5.36 (m, 2 H, =CH₂ *trans*), 5.24–5.19 (m, 2 H, =CH₂ *cis*), 4.65–4.61 (m, 4 H, CH₂ *allylic*), 4.56–4.45 (m, 2 H, CHMe₂), 1.55 (s, 9 H, CO₂CMe₃), 1.28 (d, *J* = 6.2 Hz, 6 H, CHMe₂), 1.26 (d, *J* = 6.2 Hz, 6 H, CHMe₂) ppm; ¹³C-NMR (100 MHz, DMSO-*d*₆): δ = 165.3 (q, C=O), 164.6 (q, C=O), 164.5 (q, C=O), 164.4 (q, C=O), 163.8 (q, C=O), 149.7 (Ar-C), 149.5 (Ar-C), 149.4 (Ar-C), 149.3 (Ar-C), 143.7 (Ar-C), 143.0 (Ar-C), 142.7 (Ar-C), 142.6 (Ar-C), 142.2 (Ar-C), 139.8 (Ar-C), 135.7 (Ar-C), 134.9 (Ar-C), 133.7 (t, =CH–), 133.7 (t, =CH–), 130.1 (Ar-C), 129.3 (Ar-C), 129.1 (Ar-C), 128.8 (Ar-C), 128.5 (Ar-C), 128.3 (Ar-C), 128.3 (Ar-C), 127.1 (Ar-C), 126.0 (Ar-C), 123.8 (Ar-C), 123.6 (Ar-C), 123.6 (Ar-C), 123.5 (Ar-C), 120.4 (Ar-C), 119.7 (Ar-C), 118.8 (Ar-C), 117.8 (s, =CH₂), 117.8 (s, =CH₂), 80.3 (q, CO₂CMe₃), 76.3 (t, CHMe₂), 76.3 (t, CHMe₂), 74.3 (s, CH₂ *allylic*), 74.3 (s, CH₂ *allylic*), 27.9 (p, CO₂CMe₃), 22.4 (p, CHMe₂), 22.3 (p, CHMe₂) ppm; HRMS (ESI): *m/z* calculated for C₅₈H₅₈N₆O₁₃Na [M + Na]⁺: 1069.3960; found: 1069.3964; R_f (PE/EtOAc = 1/1): 0.19.

Hexaarene 12a

Tetrakis(triphenylphosphine)palladium(0) (18 mg, 15 μ mol, 10 mol%) was added in one portion to a stirred solution of amide **17** (160 mg, 153 μ mol, 1.00 eq.) and aniline (0.05 mL, 0.50 mmol, 3.30 eq.) in THF (6.6 mL). After stirring for 90 min, the mixture was concentrated in the presence of silica gel *in vacuo*. Flash column chromatography (PE/EtOAc = 1/1 – 1/2 – 0/1) afforded phenol **S2** (66 mg, 69 μ mol, 45%) as a colorless foam.

¹H-NMR (600 MHz, DMSO-*d*₆): δ = 12.29 (bs, 2 H, OH), 10.63 (bs, 2 H, CONH), 10.51 (s, 1 H, CONH), 10.00 (s, 1 H, CONH), 9.43 (s, 1 H, CONH), 8.40 (d, *J* = 8.7 Hz, 2 H, Ar-*H*), 8.20 (d, *J* = 8.7 Hz, 2 H, Ar-*H*), 8.05 (d, *J* = 8.7 Hz, 2 H, Ar-*H*), 8.00 (pseudo s, 2 H, Ar-*H*), 7.93 (d, *J* = 8.7 Hz, 2 H, Ar-*H*), 7.91 (d, *J* = 8.7 Hz, 2 H, Ar-*H*), 7.86 (d, *J* = 8.7 Hz, 2 H, Ar-*H*), 7.64–7.61 (m, 3 H, Ar-*H*), 7.57–7.55 (m, 3 H, Ar-*H*), 4.60–4.51 (m, 2 H, CHMe₂), 1.56 (s, 9 H, CO₂CMe₃), 1.29 (d, *J* = 6.1 Hz, 6 H, CHMe₂), 1.26 (d, *J* = 6.1 Hz, 6 H, CHMe₂) ppm; ¹³C-NMR (150 MHz, DMSO-*d*₆): δ = 168.4 (q, C=O), 168.3 (q, C=O), 165.3 (q, C=O), 164.6 (q, C=O), 164.2 (q, C=O), 163.7 (q, C=O), 154.3 (q, COH), 154.1 (q, COH), 149.4 (Ar-C), 142.8 (Ar-C), 139.8 (Ar-C), 137.8 (Ar-C), 136.4 (Ar-C), 133.1 (Ar-C), 132.4 (Ar-C), 132.0 (Ar-C), 132.0 (Ar-C), 131.5 (Ar-C), 131.4 (Ar-C), 130.1 (Ar-C), 129.9 (Ar-C), 129.4 (Ar-C), 129.1 (Ar-C), 128.8 (Ar-C), 128.7 (Ar-C), 128.7 (Ar-C), 128.6 (Ar-C), 128.2 (Ar-C), 123.8 (Ar-C), 122.8 (Ar-C), 122.7 (Ar-C), 120.7 (Ar-C), 120.7 (Ar-C), 119.7 (Ar-C), 80.5 (q, CO₂CMe₃), 74.8 (t, CHMe₂), 74.8 (t, CHMe₂), 27.8 (p, CO₂CMe₃), 22.3 (p, CHMe₂), 22.3 (p, CHMe₂) ppm; HRMS (ESI): *m/z* calculated for C₅₂H₅₀N₆O₁₃Na [M+Na]⁺: 989.3334; found: 989.3335; R_f (PE/EtOAc = 1/5): 0.45.

Ester **S2** (60 mg, 62 μ mol, 1.00 eq.) was dissolved in trifluoroacetic acid (4.1 mL) at 0 °C. After stirring at room temperature for 30 min, the mixture was cooled to 0 °C. Then, Et₂O (30 mL) was poured into the reaction mixture. The resulting precipitate was filtered, washed with an excess of Et₂O, and dried *in vacuo* to furnish carboxylic acid **12a** (42 mg, 46 μ mol, 74%) as a colorless foam.

¹H-NMR (400 MHz, DMSO-*d*₆): δ = 12.81 (bs, 1 H, CO₂H), 12.30 (s, 2 H, OH), 10.65 (bs, 1 H, CONH), 10.61 (bs, 1 H, CONH), 10.51 (s, 1 H, CONH), 10.00 (s, 1 H, CONH), 9.44 (s, 1 H, CONH), 8.41–8.40 (m, 2 H, Ar-*H*), 8.21–8.19 (m, 2 H, Ar-*H*), 8.06–8.04 (m, 2 H, Ar-*H*), 8.02–7.97 (m, 6 H, Ar-*H*), 7.92–7.90 (m, 2 H, Ar-*H*), 7.88–7.85 (m, 4 H, Ar-*H*), 7.72 (d, *J* = 8.6 Hz, 1 H, Ar-*H*), 7.57 (d, *J* = 7.6 Hz, 1 H, Ar-*H*), 4.60–4.51 (m, 2 H, CHMe₂), 1.29 (d, *J* = 6.1 Hz, 6 H, CHMe₂), 1.26 (d, *J* = 6.2 Hz, 6 H, CHMe₂) ppm; ¹³C-NMR (150 MHz, DMSO-*d*₆): δ = 168.5 (q, CONH), 168.3 (q, CONH), 166.9 (q, CO₂H), 165.3 (q, CONH), 164.3 (q, CONH), 163.7 (q, CONH), 154.1 (q, COH), 154.1 (q, COH), 149.4 (Ar-C), 142.8 (Ar-C), 142.0 (Ar-C), 141.1 (Ar-C), 139.8 (Ar-C), 137.8 (Ar-C), 137.0 (Ar-C), 136.3 (Ar-C), 130.2 (Ar-C), 129.4 (Ar-C), 129.1 (Ar-C), 128.7 (Ar-C), 128.6 (Ar-C), 128.2 (Ar-C), 126.3 (Ar-C), 126.3 (Ar-C), 123.8 (Ar-C), 123.6 (Ar-C), 122.8 (Ar-C), 122.7 (Ar-C), 120.7 (Ar-C), 119.7 (Ar-C), 113.6 (Ar-C), 113.5 (Ar-C), 112.5 (Ar-C), 112.2 (Ar-C), 74.9 (t, CHMe₂), 74.9 (t, CHMe₂), 22.3 (p, CHMe₂), 22.3 (p, CHMe₂) ppm; HRMS (ESI): *m/z* calculated for C₄₈H₄₁N₆O₁₃ [M-H]⁻: 909.2732; found: 909.2735; R_f (3% MeOH/CH₂Cl₂): 0.00.

Hexaarene 18

Zinc dust (48 mg, 0.73 mmol, 2.00 eq.) was added in one portion to a stirred solution of amide **17** (380 mg, 0.36 mmol, 1.00 eq.) and glacial acetic acid (0.14 mL) in THF (0.62 mL) and ethanol (0.53 mL). After stirring vigorously for 30 min, further 2.00 eq. of zinc dust were added in one portion to the reaction mixture. That was repeated twice (ending up with 8.00 eq. of zinc dust in total for now). After stirring at 70 °C for 30 min, further 2.00 eq. of zinc dust were added in one portion and the mixture was stirred at 70 °C for 30 min. After cooling to room temperature, the reaction mixture

was diluted with EtOAc and sat. aq. NaHCO₃ was added. The precipitate was filtered, the phases were separated, and the aqueous phases was extracted with EtOAc (3×10 mL). The combined organic phases were washed with brine (5 mL), dried over MgSO₄, filtered, and concentrated in the presence of silica gel *in vacuo*. Flash column chromatography (PE/EtOAc = 1/5) afforded amine **18** (267 mg, 0.26 mmol, 73%) as a pale yellow foam.

¹H-NMR (500 MHz, DMSO-*d*₆): δ = 10.54 (s, 1 H, CONH), 10.49 (s, 1 H, CONH), 10.45 (s, 1 H, CONH), 9.56 (s, 1 H, CONH), 9.06 (s, 1 H, CONH), 8.03–7.96 (m, 7 H, Ar-*H*), 7.91–7.88 (m, 4 H, Ar-*H*), 7.84–7.83 (m, 3 H, Ar-*H*), 7.70 (d, *J* = 8.7 Hz, 2 H, Ar-*H*), 7.44–7.41 (m, 2 H, Ar-*H*), 6.64 (d, *J* = 8.6 Hz, 2 H, Ar-*H*), 6.09–5.99 (m, 2 H, =CH–), 5.88 (bs, 2 H, NH₂), 5.43–5.36 (m, 2 H, =CH₂ *trans*), 5.25–5.20 (m, 2 H, =CH₂ *cis*), 4.63–4.61 (m, 4 H, CH₂ *allylic*), 4.57–4.47 (m, 2 H, CHMe₂), 1.55 (s, 9 H, CO₂CMe₃), 1.30–1.27 (m, 12 H, CHMe₂) ppm; ¹³C-NMR (125 MHz, DMSO-*d*₆): δ = 165.3 (q, C=O), 164.6 (q, C=O), 164.5 (q, C=O), 164.5 (q, C=O), 164.4 (q, C=O), 152.6 (Ar-C), 149.5 (Ar-C), 149.4 (Ar-C), 143.0 (Ar-C), 142.7 (Ar-C), 142.6 (Ar-C), 142.2 (Ar-C), 141.2 (Ar-C), 136.4 (Ar-C), 135.7 (Ar-C), 133.7 (t, =CH–), 133.7 (t, =CH–), 130.1 (Ar-C), 129.2 (Ar-C), 129.0 (Ar-C), 128.8 (Ar-C), 128.5 (Ar-C), 128.3 (Ar-C), 127.1 (Ar-C), 126.0 (Ar-C), 125.8 (Ar-C), 123.9 (Ar-C), 123.6 (Ar-C), 120.0 (Ar-C), 119.6 (Ar-C), 119.4 (Ar-C), 119.0 (Ar-C), 118.8 (Ar-C), 117.8 (s, =CH₂), 117.8 (s, =CH₂), 117.4 (Ar-C), 112.9 (Ar-C), 80.3 (q, CO₂CMe₃), 76.3 (t, CHMe₂), 76.2 (t, CHMe₂), 74.3 (s, CH₂ *allylic*), 74.3 (s, CH₂ *allylic*), 27.9 (p, CO₂CMe₃), 22.4 (p, CHMe₂), 22.4 (p, CHMe₂) ppm; HRMS (ESI): *m/z* calculated for C₅₈H₆₁N₆O₁₁ [M+H]⁺: 1017.4398; found: 1017.4403; R_f (PE/EtOAc = 1/5): 0.52.

Hexaarene 12b

Tetrakis(triphenylphosphine)palladium(0) (13 mg, 11 μ mol, 10 mol%) was added in one portion to a stirred solution of amide **18** (110 mg, 110 μ mol, 1.00 eq.) and aniline (0.04 mL, 0.36 mmol, 3.30 eq.) in THF (4.8 mL). After stirring for 90 min, the mixture was concentrated in the presence of silica gel *in vacuo*. Flash column chromatography (PE/EtOAc = 1/5) afforded phenol **S3** (91 mg, 97 μ mol, 88%) as a colorless foam.

¹H-NMR (600 MHz, DMSO-*d*₆): δ = 12.45 (bs, 1 H, OH), 12.30 (bs, 1 H, OH), 10.62 (bs, 2 H, CONH), 10.51 (s, 1 H, CONH), 9.43 (s, 1 H, CONH), 8.98 (s, 1 H, CONH), 8.05–8.03 (m, 2 H, Ar-*H*), 8.00–7.99 (m, 4 H, Ar-*H*), 7.95–7.90 (m, 4 H, Ar-*H*), 7.87–7.84 (m, 4 H, Ar-*H*), 7.76 (d, *J* = 8.6 Hz, 1 H, Ar-*H*), 7.71 (d, *J* = 8.8 Hz, 1 H, Ar-*H*), 7.67 (d, *J* = 8.7 Hz, 2 H, Ar-*H*), 6.65 (d, *J* = 8.6 Hz, 2 H, Ar-*H*), 5.91 (s, 2 H, NH₂), 4.64–4.54 (m, 2 H, CHMe₂), 1.56 (s, 9 H, CO₂CMe₃), 1.29 (d, *J* = 2.7 Hz, 6 H, CHMe₂), 1.28 (d, *J* = 2.7 Hz, 6 H, CHMe₂) ppm; ¹³C-NMR (150 MHz, DMSO-*d*₆): δ = 169.2 (q, C=O), 168.9 (q, C=O), 165.8 (q, C=O), 165.0 (q, C=O), 164.8 (q, C=O), 164.7 (q, C=O), 154.6 (COH), 154.6 (COH), 153.2 (Ar-C), 143.3 (Ar-C), 142.5 (Ar-C), 141.6 (Ar-C), 138.2 (Ar-C), 137.5 (Ar-C), 136.8 (Ar-C), 135.4 (Ar-C), 130.4 (Ar-C), 130.0 (Ar-C), 129.4 (Ar-C), 129.1 (Ar-C), 129.0 (Ar-C), 128.7 (Ar-C), 127.3 (Ar-C), 123.3 (Ar-C), 121.3 (Ar-C), 121.1 (Ar-C), 120.4 (Ar-C), 120.2 (Ar-C), 120.2 (Ar-C), 119.6 (Ar-C), 113.4 (Ar-C), 113.0 (Ar-C), 111.7 (Ar-C), 111.2 (Ar-C), 81.0 (q, CO₂CMe₃), 75.3 (t, CHMe₂), 75.1 (t, CHMe₂), 28.3 (p, CO₂CMe₃), 22.8 (p, CHMe₂), 22.8 (p, CHMe₂) ppm; HRMS (ESI): *m/z* calculated for C₅₂H₅₁N₆O₁₁ [M-H]⁻: 935.3616; found: 935.3609; R_f (PE/EtOAc = 1/5): 0.22.

Ester **S3** (55 mg, 59 μ mol, 1.00 eq.) was dissolved in trifluoroacetic acid (3.5 mL) at 0 °C. After stirring at room temperature for 30 min, the mixture was cooled to 0 °C. Then, Et₂O (30 mL) was poured into the reaction mixture. The resulting precipitate was filtered, washed with an excess of Et₂O, and dried *in vacuo* to furnish carboxylic acid **12b** (88 mg, 27 μ mol, 46%) as a colorless foam.

¹H-NMR (500 MHz, DMSO-*d*₆): δ = 12.81 (bs, 1 H, CO₂H), 12.46 (s, 1 H, OH), 12.30 (s, 1 H, OH), 10.61 (s, 1 H, CONH), 10.60 (s, 1 H, CONH),

10.52 (s, 1 H, CONH), 9.45 (s, 1 H, CONH), 8.99 (s, 1 H, CONH), 8.05–8.03 (m, 2 H, Ar-H), 8.02–7.95 (m, 6 H, Ar-H), 7.93–7.84 (m, 7 H, Ar-H), 7.72 (d, $J=8.9$ Hz, 1 H, Ar-H), 7.68–7.66 (m, 2 H, Ar-H), 6.65–6.64 (m, 2 H, Ar-H), 5.92 (bs, 2 H, NH₂), 4.64–4.52 (m, 2 H, CHMe₂), 1.29 (d, $J=6.1$ Hz, 6 H, CHMe₂), 1.29 (d, $J=6.1$ Hz, 6 H, CHMe₂) ppm.

¹³C-NMR (125 MHz, DMSO-*d*₆): $\delta=168.7$ (q, CONH), 168.5 (q, CONH), 166.9 (q, CO₂H), 165.3 (q, CONH), 164.4 (q, CONH), 164.3 (q, CONH), 154.1 (q, COH), 154.1 (q, COH), 152.8 (Ar-C), 142.8 (Ar-C), 142.0 (Ar-C), 141.1 (Ar-C), 137.7 (Ar-C), 137.1 (Ar-C), 136.4 (Ar-C), 135.0 (Ar-C), 130.2 (Ar-C), 130.1 (Ar-C), 129.0 (Ar-C), 128.7 (Ar-C), 128.5 (Ar-C), 128.3 (Ar-C), 126.3 (Ar-C), 122.9 (Ar-C), 120.8 (Ar-C), 120.7 (Ar-C), 119.9 (Ar-C), 119.7 (Ar-C), 119.4 (Ar-C), 113.0 (Ar-C), 112.5 (Ar-C), 112.3 (Ar-C), 111.2 (Ar-C), 110.8 (Ar-C), 74.9 (t, CHMe₂), 74.7 (t, CHMe₂), 22.4 (p, CHMe₂), 22.3 (p, CHMe₂) ppm.

HRMS (ESI): m/z calculated for C₄₈H₄₃N₆O₁₁ [M-H]⁻: 879.2990; found: 879.2989. R_f (3% MeOH/CH₂Cl₂): 0.00.

Hexaarene 12c

Mercury(II) chloride (88 mg, 0.32 mmol, 1.10 eq.) was added to a stirred solution of amine **18** (300 mg, 0.29 mmol, 1.00 eq.), 1,3-bis(*tert*-butoxycarbonyl)-2-methyl-2-thiopseudourea (**19**) (94 mg, 0.32 mmol, 1.10 eq.), and Et₃N (0.09 mL, 0.65 mmol, 2.20 eq.) in DMF (15 mL) at 0°C. After stirring at 0°C for 3 h, the mixture was stirred at room temperature for a further 24 h. Subsequently, the reaction mixture was diluted with EtOAc and filtered through a thick pad of Celite™ (washing with an excess of EtOAc). The filtrate was washed with water (100 mL) and brine (100 mL), dried over MgSO₄, filtered, and concentrated *in vacuo*. Flash column chromatography (washing with 100% CH₂Cl₂, eluting with 3% MeOH/CH₂Cl₂) afforded amide **S4** (324 mg, 0.26 mmol, 89%) as a yellow foam.

¹H-NMR (600 MHz, DMSO-*d*₆): $\delta=11.28$ (s, 1 H, NH), 10.53 (s, 2 H, NH), 10.45 (s, 1 H, NH), 10.19 (s, 1 H, NH), 9.63 (s, 1 H, NH), 9.55 (s, 1 H, NH), 8.05–7.94 (m, 8 H, Ar-H), 7.92–7.87 (m, 4 H, Ar-H), 7.84–7.75 (m, 6 H, Ar-H), 7.44–7.40 (m, 2 H, Ar-H), 6.08–5.99 (m, 2 H, -CH=), 5.43–5.36 (m, 2 H, =CH₂ *trans*), 5.24–5.19 (m, 2 H, =CH₂ *cis*), 4.66–4.58 (m, 4 H, CH₂ *allylic*), 4.55–4.47 (m, 2 H, CHMe₂), 1.55 (s, 9 H, CO₂CMe₃), 1.52 (s, 9 H, NCO₂CMe₃), 1.44 (s, 9 H, NCO₂CMe₃), 1.29–1.25 (m, 12 H, CHMe₂) ppm.

¹³C-NMR (150 MHz, DMSO-*d*₆): $\delta=165.3$ (q, C=O), 164.6 (q, C=O), 164.5 (q, C=O), 164.3 (q, C=O), 164.3 (q, C=O), 152.0 (q, C=N), 149.6 (q, NCO₂), 149.5 (q, NCO₂), 143.0 (Ar-C), 142.8 (Ar-C), 142.5 (Ar-C), 140.3 (Ar-C), 135.7 (Ar-C), 135.6 (Ar-C), 133.7 (t, =CH-), 133.6 (t, =CH-), 130.1 (Ar-C), 129.9 (Ar-C), 129.6 (Ar-C), 129.0 (Ar-C), 128.8 (Ar-C), 128.5 (Ar-C), 128.5 (Ar-C), 128.3 (Ar-C), 128.3 (Ar-C), 127.3 (Ar-C), 127.1 (Ar-C), 126.0 (Ar-C), 123.6 (Ar-C), 122.9 (Ar-C), 121.7 (Ar-C), 119.6 (Ar-C), 119.4 (Ar-C), 119.3 (Ar-C), 119.0 (Ar-C), 118.8 (Ar-C), 118.7 (Ar-C), 112.9 (Ar-C), 117.8 (s, =CH₂), 117.8 (s, =CH₂), 81.8 (q, NCO₂CMe₃), 80.3 (q, CO₂CMe₃), 79.1 (q, NCO₂CMe₃), 76.2 (t, CHMe₂), 76.2 (t, CHMe₂), 74.3 (s, CH₂ *allylic*), 74.3 (s, CH₂ *allylic*), 27.8 (p, CO₂CMe₃), 27.7 (p, NCO₂CMe₃), 27.6 (p, NCO₂CMe₃), 22.3 (p, CHMe₂), 22.3 (p, CHMe₂) ppm; HRMS (ESI): m/z calculated for C₆₉H₇₉N₈O₁₅ [M+H]⁺: 1259.5665; found: 1259.5642; R_f (PE/EtOAc = 1/5): 0.77.

Tetrakis(triphenylphosphine)palladium(0) (9 mg, 8 μ mol, 0.10 eq.) was added in one portion to a stirred solution of ether **S4** (100 mg, 0.08 mmol, 1.00 eq.) and aniline (24 μ L, 0.26 mmol, 3.30 eq.) in THF (3.5 mL). After 90 min, the mixture was concentrated in the presence of silica gel *in vacuo*. Flash column chromatography (washing with PE/EtOAc = 1/1, then eluting with 5% MeOH/CH₂Cl₂) afforded phenol **S5** (47 mg, 0.04 mmol, 50%) as a yellow foam.

¹H-NMR (600 MHz, DMSO-*d*₆): $\delta=12.33$ (bs, 1 H, OH), 12.29 (bs, 1 H, OH), 11.27 (s, 1 H, NH), 10.62 (bs, 2 H, NH), 10.51 (s, 1 H, NH), 10.19 (s, 1 H, NH), 9.48 (bs, 1 H, NH), 9.42 (bs, 1 H, NH), 8.05–7.85 (m, 12 H, Ar-H), 7.64–7.54 (m, 8 H, Ar-H), 4.63–4.53 (m, 2 H, CHMe₂), 1.56 (s, 9 H, CO₂CMe₃), 1.52 (s, 9 H, NCO₂CMe₃), 1.43 (s, 9 H, NCO₂CMe₃), 1.29–1.27 (m, 12 H, CHMe₂) ppm;

¹³C-NMR (150 MHz, DMSO-*d*₆): $\delta=168.4$ (q, C=O), 165.3 (q, C=O), 164.6 (q, C=O), 164.3 (q, C=O), 162.3 (q, C=O), 162.2 (q, C=O), 154.2 (q, C=N), 152.1 (q, COH), 152.0 (q, COH), 149.6 (q, NCO₂), 149.5 (q, NCO₂), 142.8 (Ar-C), 136.4 (Ar-C), 133.0 (Ar-C), 132.4 (Ar-C), 132.1 (Ar-C), 132.1 (Ar-C), 131.5 (Ar-C), 131.5 (Ar-C), 130.2 (Ar-C), 130.1 (Ar-C), 129.9 (Ar-C), 129.3 (Ar-C), 128.7 (Ar-C), 128.7 (Ar-C), 128.5 (Ar-C), 128.2 (Ar-C), 123.0 (Ar-C), 122.9 (Ar-C), 122.8 (Ar-C), 121.8 (Ar-C), 120.7 (Ar-C), 120.0 (Ar-C), 119.8 (Ar-C), 119.0 (Ar-C), 113.0 (Ar-C), 112.6 (Ar-C), 83.4 (q, NCO₂CMe₃), 80.5 (q, CO₂CMe₃), 79.1 (q, NCO₂CMe₃), 74.9 (t, CHMe₂), 74.8 (t, CHMe₂), 27.9 (p, CO₂CMe₃), 27.9 (p, NCO₂CMe₃), 27.7 (p, NCO₂CMe₃), 22.4 (p, CHMe₂), 22.4 (p, CHMe₂) ppm; HRMS (ESI): m/z calculated for C₆₃H₆₉N₈O₁₅ [M-H]⁻: 1177.4882; found: 1177.4889; R_f (PE/EtOAc = 1/5): 0.29.

Ester **S5** (40 mg, 34 μ mol, 1.00 eq.) was dissolved in trifluoroacetic acid (2 mL) at 0°C. After stirring at room temperature for 30 min, the mixture was cooled to 0°C. Then, Et₂O (20 mL) was poured into the reaction mixture. The resulting precipitate was filtered, washed with an excess of Et₂O, and dried *in vacuo* to furnish carboxylic acid **12c** (27 mg, 29 μ mol, 86%) as a yellow foam.

¹H-NMR (600 MHz, DMSO-*d*₆): $\delta=12.81$ (bs, 1 H, CO₂H), 12.39 (s, 1 H, OH), 12.30 (s, 1 H, OH), 10.64 (s, 1 H, NH), 10.61 (s, 1 H, NH), 10.52 (s, 1 H, NH), 9.94 (s, 1 H, NH), 9.55 (s, 1 H, NH), 9.44 (s, 1 H, NH), 8.06–7.85 (m, 18 H, 1 NH, Ar-H), 7.72 (d, $J=8.8$ Hz, 1 H, Ar-H), 7.67 (d, $J=8.5$ Hz, 1 H, Ar-H), 7.63 (bs, 2H, NH₂), 7.42 (d, $J=8.5$ Hz, 1 H, Ar-H), 4.61–4.53 (m, 2 H, CHMe₂), 1.29–1.27 (m, 12 H, CHMe₂) ppm; ¹³C-NMR (150 MHz, DMSO-*d*₆): $\delta=168.5$ (q, CONH), 166.9 (q, CO₂H), 165.3 (q, CONH), 165.3 (q, CONH), 164.3 (q, CONH), 164.0 (q, CONH), 155.4 (q, HNC(=NH)NH₂), 154.2 (q, COH), 154.1 (q, COH), 142.0 (Ar-C), 137.1 (Ar-C), 136.7 (Ar-C), 136.3 (Ar-C), 130.2 (Ar-C), 129.0 (Ar-C), 128.7 (Ar-C), 128.6 (Ar-C), 128.3 (Ar-C), 128.2 (Ar-C), 126.3 (Ar-C), 123.3 (Ar-C), 123.0 (Ar-C), 122.8 (Ar-C), 122.8 (Ar-C), 120.8 (Ar-C), 120.7 (Ar-C), 119.9 (Ar-C), 119.8 (Ar-C), 119.4 (Ar-C), 117.1 (Ar-C), 113.0 (Ar-C), 112.7 (Ar-C), 112.6 (Ar-C), 112.4 (Ar-C), 112.2 (Ar-C), 74.9 (t, CHMe₂), 74.9 (t, CHMe₂), 22.4 (p, CHMe₂), 22.3 (p, CHMe₂) ppm; HRMS (ESI): m/z calculated for C₄₉H₄₅N₈O₁₁ [M-H]⁻: 921.3208; found: 921.3219.

„Dimer“ 21

Amine **18** (750 mg, 0.74 mmol, 1.00 eq.), carboxylic acid **20** (330 mg, 1.25 mmol, 1.70 eq.), and EEDQ (283 mg, 1.14 mmol, 1.55 eq.) were added to precooled CHCl₃ (3.8 mL) at 0°C. Subsequently, the reaction mixture was stirred for 24 h while slowly warming up to room temperature. After concentrating under reduced pressure in the presence of silica gel, flash column chromatography (washing with 20% Et₂O/CH₂Cl₂, eluting with 3% MeOH/CH₂Cl₂) afforded amide **21** (476 mg, 0.38 mmol, 51%) as a yellow foam.

¹H-NMR (400 MHz, DMSO-*d*₆): $\delta=10.53$ (s, 2 H, CONH), 10.45 (s, 1 H, CONH), 10.36 (s, 1 H, CONH), 9.56 (s, 1 H, CONH), 9.52 (s, 1 H, CONH), 8.03–7.79 (m, 19 H, Ar-H), 7.45–4.0 (m, 3 H, 1 Ar-H, CONH₂), 6.86–6.79 (m, 1 H, NHBoc), 6.10–5.97 (m, 2 H, -CH=), 5.43–5.35 (m, 2 H, =CH₂ *trans*), 5.24–5.19 (m, 2 H, =CH₂ *cis*), 4.64–4.61 (m, 4 H, CH₂ *allylic*), 4.51 (septet, $J=6.0$ Hz, 2 H, CHMe₂), 4.40 (t, $J=7.4$ Hz, 1 H, CHNH), 3.85 (d, $J=7.1$ Hz, 1 H, CHOME), 3.32 (s, 3 H, OMe), 1.55 (s, 9 H, CO₂CMe₃), 1.38 (s, 9 H, NHCO₂CMe₃), 1.28 (d, $J=6.1$ Hz, 6 H, CHMe₂), 1.27 (d, $J=6.0$ Hz, 6 H, CHMe₂) ppm; ¹³C-NMR (150 MHz, DMSO-*d*₆): $\delta=170.6$ (q, CONH₂), 165.3 (q, CO₂CMe₃), 164.6 (q,

CONH), 164.5 (q, CONH), 164.5 (q, CONH), 164.4 (q, CONH), 164.3 (q, CONH), 164.3 (q, CONH), 154.8 (q, HNCOC₂Me₃), 149.5 (Ar–C), 149.5 (Ar–C), 143.0 (Ar–C), 142.7 (Ar–C), 142.6 (Ar–C), 142.5 (Ar–C), 142.2 (Ar–C), 135.7 (Ar–C), 133.7 (t, =CH–), 133.6 (t, =CH–), 130.1 (Ar–C), 129.9 (Ar–C), 129.2 (Ar–C), 129.0 (Ar–C), 128.8 (Ar–C), 128.7 (Ar–C), 128.6 (Ar–C), 128.5 (Ar–C), 128.4 (Ar–C), 128.4 (Ar–C), 128.3 (Ar–C), 127.1 (Ar–C), 126.0 (Ar–C), 123.7 (Ar–C), 123.6 (Ar–C), 123.6 (Ar–C), 119.6 (Ar–C), 119.4 (Ar–C), 119.0 (Ar–C), 118.8 (Ar–C), 117.8 (s, =CH₂), 117.8 (s, =CH₂), 80.3 (q, CO₂CMe₃), 80.1 (q, HNCOC₂Me₃), 78.7 (t, CHOMe), 76.2 (t, CHMe₂), 76.2 (t, CHMe₂), 74.3 (s, CH₂ allylic), 74.3 (CH₂ allylic), 57.6 (p, OMe), 56.6 (t, CHNH), 28.1 (p, HNCOC₂Me₃), 27.9 (p, CO₂CMe₃), 22.3 (p, CHMe₂), 22.3 (p, CHMe₂) ppm; HRMS (ESI): m/z calculated for C₆₈H₇₇N₈O₁₆ [M+H]⁺: 1261.5458; found: 1261.5458; [α]_D²⁷ = –78.0° (c 0.2, DMSO-d₆); R_f (PE/EtOAc = 1/5): 0.07.

“Extended” cystobactamid derivative 13b

HCl (8 mL, 4 M in 1,4-dioxane, 32 mmol, 100 eq.) was added to amide **21** (400 mg, 0.32 mmol, 1.00 eq.) at 0 °C. The solution was warmed up to room temperature (over a period of 5 min) and stirred for further 15 min. Then, the reaction mixture was poured into a vigorously stirred mixture of EtOAc (120 mL) and sat. aq. NaHCO₃ (120 mL). The phases were separated, the aqueous phase was extracted with EtOAc (3×120 mL), the combined organic phases were washed with brine, dried over MgSO₄, filtered, and concentrated *in vacuo* to afford the corresponding crude amine **22**.

Next, DIPEA (0.36 mL, 2.08 mmol, 13.0 eq.) was added dropwise to a solution of carboxylic acid **23b** (107 mg, 0.40 mmol, 2.50 eq.) and HATU (152 mg, 0.40 mmol, 2.50 eq.) in DMF (3.8 mL). After 5 min, the resulting mixture was slowly transferred to a solution of the crude product from above **22** (186 mg, 0.16 mmol, 1.00 eq.) in DMF (2.2 mL) at 0 °C. Then, the reaction mixture was stirred for 15 h while slowly warming up to room temperature. Next, the mixture was diluted with EtOAc (10 mL), washed with aq. HCl (12 mL, 0.1 M), aq. NaCl (5×10 mL, 5% sat.), dried over MgSO₄, filtered, and concentrated in the presence of silica gel *in vacuo*. Flash column chromatography (washing with 2% MeOH/CH₂Cl₂, eluting with 4% MeOH/CH₂Cl₂) afforded amide **S6** (109 mg, 77 μmol, 48% o/s) as a yellow foam.

¹H-NMR (600 MHz, DMSO-d₆): δ = 10.72 (s, 1 H, CONH), 10.56 (s, 1 H, CONH), 10.53 (s, 2 H, CONH), 10.45 (s, 1 H, CONH), 9.55 (s, 1 H, CONH), 9.53 (s, 1 H, CONH), 8.45 (d, J = 8.2 Hz, 1 H, CONH), 8.13–8.11 (m, 2 H, Ar-H), 8.05–7.97 (m, 12 H, Ar-H), 7.91–7.88 (m, 7 H, Ar-H), 7.85–7.83 (m, 5 H, Ar-H), 7.54 (bs, 1 H, CONH₂), 7.47 (bs, 1 H, CONH₂), 7.44 (d, J = 8.5 Hz, 1 H, Ar-H), 7.42 (d, J = 8.5 Hz, 1 H, Ar-H), 6.08–5.99 (m, 2 H, -CH=), 5.42–5.36 (m, 2 H, =CH₂ trans), 5.24–5.20 (m, 2 H, =CH₂ cis), 4.92 (t, J = 8.1 Hz, 1 H, CHNH), 4.64–4.62 (m, 4 H, CH₂ allylic), 4.51 (septet, J = 5.6 Hz, 2 H, CHMe₂), 4.09 (d, J = 8.2 Hz, 1 H, CHOMe), 3.32 (s, 3 H, OMe), 1.55 (s, 9 H, CO₂CMe₃), 1.28 (d, J = 6.0 Hz, 6 H, CHMe₂), 1.27 (d, J = 6.0 Hz, 6 H, CHMe₂) ppm; ¹³C-NMR (150 MHz, DMSO-d₆): δ = 170.9 (q, CONH₂), 168.7 (q, CONH), 167.3 (q, CONH), 165.5 (q, CONH), 165.3 (q, CO₂CMe₃), 164.6 (q, CONH), 164.5 (q, CONH), 164.5 (q, CONH), 164.4 (q, CONH), 164.3 (q, CONH), 149.5 (Ar–C), 149.5 (Ar–C), 142.6 (Ar–C), 142.5 (Ar–C), 141.8 (Ar–C), 138.7 (Ar–C), 138.7 (Ar–C), 135.7 (Ar–C), 135.7 (Ar–C), 133.7 (t, =CH–), 133.7 (t, =CH–), 132.5 (Ar–C), 130.4 (Ar–C), 130.1 (Ar–C), 129.2 (Ar–C), 129.2 (Ar–C), 129.2 (Ar–C), 128.9 (Ar–C), 128.8 (Ar–C), 128.6 (Ar–C), 128.6 (Ar–C), 128.5 (Ar–C), 128.4 (Ar–C), 128.4 (Ar–C), 128.3 (Ar–C), 128.3 (Ar–C), 127.1 (Ar–C), 126.0 (Ar–C), 123.7 (Ar–C), 123.6 (Ar–C), 119.7 (Ar–C), 119.6 (Ar–C), 119.5 (Ar–C), 119.0 (Ar–C), 118.9 (Ar–C), 118.9 (Ar–C), 118.8 (Ar–C), 118.3 (Ar–C), 117.8 (s, =CH₂), 117.8 (s, =CH₂), 114.1 (q, CN), 80.3 (q, CO₂CMe₃), 80.0 (t, CHOMe), 76.3 (t, CHMe₂), 76.3 (t, CHMe₂), 74.3 (s, CH₂ allylic), 74.3 (s, CH₂ allylic), 57.7 (p, OMe), 55.8 (t, CHNH), 27.9 (p, CO₂CMe₃), 22.4 (p, CHMe₂), 22.3 (p, CHMe₂) ppm; HRMS (ESI): m/z calculated for

C₇₈H₇₇N₁₀O₁₆ [M+H]⁺: 1409.5519; found: 1409.5520; [α]_D²⁴ = +2.5° (c 0.2, MeCN); R_f (PE/EtOAc = 1/5): 0.04.

Tetrakis(triphenylphosphine)palladium(0) (4 mg, 4 μmol, 0.10 eq.) was added in one portion to a stirred solution of ether **S6** (50 mg, 35.0 μmol, 1.00 eq.) and aniline (10 μL, 117 μmol, 3.30 eq.) in THF (1.5 mL). After 90 min, the mixture was concentrated in the presence of silica gel *in vacuo*. Flash column chromatography (washing with 0–3% MeOH/CH₂Cl₂, then eluting with 6–8% MeOH/CH₂Cl₂) afforded phenol **S7** (35 mg, 26 μmol, 75%) as a yellow foam.

¹H-NMR (600 MHz, DMSO-d₆): δ = 12.37 (bs, 1 H, OH), 12.29 (bs, 1 H, OH), 10.72 (s, 1 H, CONH), 10.62 (bs, 2 H, CONH), 10.58 (s, 1 H, CONH), 10.51 (s, 1 H, CONH), 9.43 (bs, 1 H, CONH), 9.41 (bs, 1 H, CONH), 8.46 (d, J = 8.0 Hz, 1 H, CONH), 8.13–8.11 (m, 2 H, Ar-H), 8.05–8.03 (m, 4 H, Ar-H), 7.99–7.84 (m, 22 H, Ar-H), 7.54 (bs, 1 H, CONH₂), 7.48 (bs, 1 H, CONH₂), 4.92 (t, J = 8.1 Hz, 1 H, CHNH), 4.57 (m, 2 H, CHMe₂), 4.09 (d, J = 7.9 Hz, 1 H, CHOMe), 3.31 (s, 3 H, OMe), 1.56 (s, 9 H, CO₂CMe₃), 1.29–1.27 (m, 12 H, CHMe₂) ppm; ¹³C-NMR (150 MHz, DMSO-d₆): δ = 170.9 (q, CONH₂), 168.7 (q, C=O), 168.5 (q, C=O), 166.9 (q, C=O), 165.5 (q, C=O), 165.3 (q, C=O), 164.6 (q, C=O), 164.5 (q, C=O), 164.2 (q, C=O), 164.2 (q, C=O), 154.2 (q, COH), 154.2 (q, COH), 142.8 (Ar–C), 142.3 (Ar–C), 141.8 (Ar–C), 138.7 (Ar–C), 138.7 (Ar–C), 137.0 (Ar–C), 136.4 (Ar–C), 132.5 (Ar–C), 131.5 (Ar–C), 130.3 (Ar–C), 129.9 (Ar–C), 128.9 (Ar–C), 128.8 (Ar–C), 128.7 (Ar–C), 128.7 (Ar–C), 128.7 (Ar–C), 128.6 (Ar–C), 128.6 (Ar–C), 128.6 (Ar–C), 128.3 (Ar–C), 128.3 (Ar–C), 128.2 (Ar–C), 122.9 (Ar–C), 122.9 (Ar–C), 122.8 (Ar–C), 120.8 (Ar–C), 120.7 (Ar–C), 120.3 (Ar–C), 119.7 (Ar–C), 119.6 (Ar–C), 119.6 (Ar–C), 119.4 (Ar–C), 119.0 (Ar–C), 118.3 (Ar–C), 114.1 (Ar–C), 80.5 (q, CO₂CMe₃), 80.0 (t, CHOMe), 74.9 (t, CHMe₂), 74.9 (t, CHMe₂), 57.8 (p, OMe), 55.8 (t, CHNH), 27.9 (p, CO₂CMe₃), 22.4 (p, CHMe₂), 22.3 (p, CHMe₂) ppm.

HRMS (ESI): m/z calculated for C₇₂H₆₇N₁₀O₁₆ [M–H][–]: 1327.4737; found: 1327.4730; [α]_D²⁸ = +19.0° (c 0.1, DMSO-d₆); R_f (10% MeOH/CH₂Cl₂): 0.64.

Ester **S7** (30 mg, 22.6 μmol, 1.00 eq.) was dissolved in trifluoroacetic acid (1.0 mL) at 0 °C. After stirring at room temperature for 30 min, the mixture was cooled to 0 °C. Then, Et₂O (10 mL) was poured into the reaction mixture. The resulting precipitate was filtered, washed with an excess of Et₂O, and dried *in vacuo* to furnish carboxylic acid **13b** (22 mg, 15.3 μmol, 68%) as a yellow foam.

¹H-NMR (600 MHz, DMSO-d₆): δ = 12.81 (bs, 1 H, CO₂H), 12.37 (s, 1 H, OH), 12.30 (s, 1 H, OH), 10.72 (s, 1 H, CONH), 10.63 (s, 1 H, CONH), 10.61 (s, 1 H, CONH), 10.58 (s, 1 H, CONH), 10.52 (s, 1 H, CONH), 9.45 (s, 1 H, CONH), 9.41 (s, 1 H, CONH), 8.46 (d, J = 8.0 Hz, 1 H, CONH), 8.13–8.12 (m, 2 H, Ar-H), 8.05–8.04 (m, 4 H, Ar-H), 8.02–7.95 (m, 9 H, Ar-H), 7.92–7.84 (m, 12 H, Ar-H), 7.73–7.71 (m, 1 H, Ar-H), 7.55 (bs, 1 H, CONH₂), 7.48 (bs, 1 H, CONH₂), 4.92 (t, J = 8.1 Hz, 1 H, CHNH), 4.60–4.52 (m, 2 H, CHMe₂), 4.09 (d, J = 8.1 Hz, 1 H, CHOMe), 3.31 (s, 3 H, OMe), 1.29–1.27 (m, 12 H, CHMe₂) ppm; ¹³C-NMR (150 MHz, DMSO-d₆): δ = 170.9 (q, CONH₂), 168.7 (q, C=O), 168.5 (q, C=O), 168.5 (q, C=O), 166.9 (q, C=O), 165.5 (q, C=O), 165.3 (q, C=O), 164.5 (q, C=O), 164.3 (q, C=O), 164.2 (q, C=O), 157.7 (q, quartet, J = 30.6 Hz, F₃CCO₂), 154.2 (q, COH), 154.1 (q, COH), 142.8 (Ar–C), 142.3 (Ar–C), 142.0 (Ar–C), 141.8 (Ar–C), 141.1 (Ar–C), 138.7 (Ar–C), 137.1 (Ar–C), 136.4 (Ar–C), 136.3 (Ar–C), 132.5 (Ar–C), 130.2 (Ar–C), 130.1 (Ar–C), 128.9 (Ar–C), 128.7 (Ar–C), 128.6 (Ar–C), 128.6 (Ar–C), 128.5 (Ar–C), 128.3 (Ar–C), 128.3 (Ar–C), 128.3 (Ar–C), 126.3 (Ar–C), 122.8 (Ar–C), 122.8 (Ar–C), 120.8 (Ar–C), 120.7 (Ar–C), 119.9 (q, quartet, J = 121.6 Hz, F₃CCO₂), 119.7 (Ar–C), 119.6 (Ar–C), 119.4 (Ar–C), 119.0 (Ar–C), 118.3 (Ar–C), 114.1 (q, CN), 112.5 (Ar–C), 112.4 (Ar–C), 112.3 (Ar–C), 112.2 (Ar–C), 80.0 (t, CHOMe), 74.9 (t, 2 C, CHMe₂), 57.8 (p, OMe), 55.8 (t, CHNH), 22.3 (p, 2 CHMe₂) ppm; HRMS (ESI): m/z calculated for C₆₈H₆₀N₁₀O₁₆Na [M+Na]⁺: 1295.4086; found:

1295.4083; $[\alpha]_D^{22} = +39.7^\circ$ (c 0.3, DMSO- d_6); R_f (10% MeOH/ CH_2Cl_2): 0.31.

"Extended" cystobactamid derivative 13a

HCl (8 mL, 4 M in 1,4-dioxane, 32.0 mmol, 100 eq.) was added to amide **21** (400 mg, 0.32 mmol, 1.00 eq.) at 0°C. The solution was warmed up to room temperature (over a period of 5 min) and stirred for further 15 min. Then, the reaction mixture was poured into a vigorously stirred mixture of EtOAc (120 mL) and sat. aq. $NaHCO_3$ (120 mL). The phases were separated, the aqueous phase was extracted with EtOAc (3x120 mL), the combined organic phases were washed with brine, dried over $MgSO_4$, filtered, and concentrated *in vacuo* to afford the corresponding crude amine **22**.

Next, DIPEA (0.36 mL, 2.08 mmol, 13.0 eq.) was added dropwise to a solution of carboxylic acid **23a** (115 mg, 0.40 mmol, 2.50 eq.) and HATU (152 mg, 0.40 mmol, 2.50 eq.) in DMF (3.8 mL). After 5 min, the resulting mixture was slowly transferred to a solution of the crude product **22** from above (186 mg, 0.16 mmol, 1.00 eq.) in DMF (2.2 mL) at 0°C. Then, the reaction mixture was stirred for 15 h while slowly warming up to room temperature. Next, the mixture was diluted with EtOAc (10 mL), washed with aq. HCl (12 mL, 0.1 M), aq. NaCl (5x10 mL, 5% sat.), dried over $MgSO_4$, filtered, and concentrated in the presence of silica gel *in vacuo*. Flash column chromatography (washing with 2% MeOH/ CH_2Cl_2 , eluting with 4% MeOH/ CH_2Cl_2) afforded amide **S8** (50 mg, 35 μ mol, 22% o2 s) as a yellow foam.

1H -NMR (400 MHz, DMSO- d_6): $\delta = 10.83$ (s, 1 H, CONH), 10.81 (s, 1 H, CONH), 10.56 (s, 1 H, CONH), 10.53 (s, 1 H, CONH), 10.46 (s, 1 H, CONH), 9.56 (s, 1 H, CONH), 9.53 (s, 1 H, CONH), 8.46 (d, $J = 7.8$ Hz, 1 H, CONH), 8.40–8.37 (m, 3 H, Ar-H), 8.22–8.18 (m, 3 H, Ar-H), 8.03–7.95 (m, 8 H, Ar-H), 7.92–7.88 (m, 8 H, Ar-H), 7.84–7.82 (m, 4 H, Ar-H), 7.55 (bs, 1 H, CONH₂), 7.48 (bs, 1 H, CONH₂), 7.45–7.41 (m, 2 H, Ar-H), 6.09–5.98 (m, 2 H, =CH=), 5.43–5.35 (m, 2 H, =CH₂ trans), 5.24–5.19 (m, 2 H, =CH₂ cis), 4.92 (t, $J = 8.0$ Hz, 1 H, CHNH), 4.64–4.61 (m, 4 H, CH₂ allylic), 4.51 (septet, $J = 6.4$ Hz, 2 H, CHMe₂), 4.09 (d, $J = 8.0$ Hz, 1 H, CHOMe), 3.31 (s, 3 H, OMe), 1.55 (s, 9 H, CO₂CMe₃), 1.28 (d, $J = 6.1$ Hz, 6 H, CHMe₂), 1.27 (d, $J = 6.1$ Hz, 6 H, CHMe₂) ppm; ^{13}C -NMR (125 MHz, DMSO- d_6): $\delta = 170.9$ (q, CONH₂), 168.7 (q, C=O), 166.9 (q, C=O), 165.5 (q, C=O), 165.3 (q, C=O), 164.6 (q, C=O), 164.5 (q, C=O), 164.4 (q, C=O), 164.3 (q, C=O), 164.3 (q, C=O), 149.6 (Ar-C), 149.3 (Ar-C), 149.3 (Ar-C), 143.1 (Ar-C), 142.8 (Ar-C), 142.6 (Ar-C), 142.6 (Ar-C), 141.8 (Ar-C), 140.4 (Ar-C), 140.3 (Ar-C), 140.3 (Ar-C), 135.7 (Ar-C), 133.7 (t, -CH=), 133.7 (t, -CH=), 130.4 (Ar-C), 130.3 (Ar-C), 130.1 (Ar-C), 129.4 (Ar-C), 129.4 (Ar-C), 129.0 (Ar-C), 128.9 (Ar-C), 128.5 (Ar-C), 128.5 (Ar-C), 128.4 (Ar-C), 128.3 (Ar-C), 127.1 (Ar-C), 126.1 (Ar-C), 123.7 (Ar-C), 123.6 (Ar-C), 119.7 (Ar-C), 119.7 (Ar-C), 119.6 (Ar-C), 119.1 (Ar-C), 119.0 (Ar-C), 118.9 (Ar-C), 118.9 (Ar-C), 118.9 (Ar-C), 117.8 (s, =CH₂), 117.8 (s, =CH₂), 109.6 (Ar-C), 80.4 (q, CO₂CMe₃), 80.0 (t, CHOMe), 76.3 (t, CHMe₂), 76.3 (t, CHMe₂), 74.3 (s, CH₂ allylic), 74.3 (s, CH₂ allylic), 57.8 (p, OMe), 55.8 (t, CHNH), 27.9 (p, CO₂CMe₃), 22.4 (p, CHMe₂), 22.4 (p, CHMe₂) ppm; HRMS (ESI): m/z calculated for C₇₇H₇₆N₁₀O₁₈Na [M+Na]⁺: 1451.5237; found: 1451.5200; $[\alpha]_D^{23} = +26.0^\circ$ (c 0.1, DMSO- d_6); R_f (10% MeOH/ CH_2Cl_2): 0.58.

Tetrakis(triphenylphosphine)palladium(0) (3 mg, 3 μ mol, 0.10 eq.) was added in one portion to a stirred solution of ether **S8** (40 mg, 28.0 μ mol, 1.00 eq.) and aniline (10 μ L, 92 μ mol, 3.30 eq.) in THF (1.2 mL). After 90 min, the mixture was concentrated in the presence of silica gel *in vacuo*. Flash column chromatography (washing with 0–3% MeOH/ CH_2Cl_2 , then eluting with 6–8% MeOH/ CH_2Cl_2) afforded phenol **S9** (19 mg, 14 μ mol, 51%) as a yellow foam.

1H -NMR (600 MHz, DMSO- d_6): $\delta = 12.37$ (bs, 1 H, OH), 12.30 (bs, 1 H, OH), 10.81 (s, 1 H, CONH), 10.62 (bs, 2 H, CONH), 10.58 (s, 1 H, CONH), 10.51 (s, 1 H, CONH), 9.43 (bs, 1 H, CONH), 9.40 (bs, 1 H, CONH), 8.47 (d, $J = 8.0$ Hz, 1 H, CONH), 8.40–8.38 (m, 2 H, Ar-H), 8.22–8.19 (m, 2 H, Ar-H), 8.05–8.04 (m, 2 H, Ar-H), 8.02–7.89 (m, 18 H, Ar-H), 7.87–7.84 (m, 4 H, Ar-H), 7.54 (bs, 1 H, CONH₂), 7.48 (bs, 1 H, CONH₂), 4.92 (t, $J = 8.0$ Hz, 1 H, CHNH), 4.60–4.54 (m, 2 H, CHMe₂), 4.10 (d, $J = 8.1$ Hz, 1 H, CHOMe), 3.32 (s, 3 H, OMe), 1.56 (s, 9 H, CO₂CMe₃), 1.29–1.27 (m, 12 H, CHMe₂) ppm; ^{13}C -NMR (150 MHz, DMSO- d_6): $\delta = 170.9$ (q, CONH₂), 168.7 (q, C=O), 168.4 (q, C=O), 165.4 (q, C=O), 165.3 (q, C=O), 164.6 (q, C=O), 164.2 (q, C=O), 164.2 (q, C=O), 164.2 (q, C=O), 154.1 (q, COH), 154.1 (q, COH), 149.3 (Ar-C), 142.8 (Ar-C), 142.3 (Ar-C), 142.2 (Ar-C), 141.7 (Ar-C), 140.3 (Ar-C), 137.0 (Ar-C), 136.4 (Ar-C), 136.4 (Ar-C), 130.3 (Ar-C), 129.9 (Ar-C), 129.3 (Ar-C), 129.0 (Ar-C), 128.7 (Ar-C), 128.6 (Ar-C), 128.6 (Ar-C), 128.5 (Ar-C), 128.5 (Ar-C), 128.3 (Ar-C), 128.2 (Ar-C), 126.7 (Ar-C), 123.6 (Ar-C), 122.9 (Ar-C), 122.8 (Ar-C), 120.7 (Ar-C), 120.6 (Ar-C), 119.7 (Ar-C), 119.7 (Ar-C), 119.6 (Ar-C), 119.4 (Ar-C), 119.0 (Ar-C), 119.0 (Ar-C), 112.5 (Ar-C), 112.1 (Ar-C), 80.5 (q, CO₂CMe₃), 80.0 (t, CHOMe), 74.8 (t, CHMe₂), 74.8 (t, CHMe₂), 57.7 (p, OMe), 55.8 (t, CHNH), 27.8 (p, CO₂CMe₃), 22.3 (p, CHMe₂), 22.3 (p, CHMe₂) ppm; HRMS (ESI): m/z calculated for C₇₁H₆₇N₁₀O₁₈ [M-H]⁻: 1347.4635; found: 1347.4630; $[\alpha]_D^{28} = -94.0^\circ$ (c 0.2, DMSO- d_6); R_f (10% MeOH/ CH_2Cl_2): 0.48.

Ester **S9** (20 mg, 15 μ mol, 1.00 eq.) was dissolved in trifluoroacetic acid (1.0 mL) at 0°C. After stirring at room temperature for 30 min, the mixture was cooled to 0°C. Then, Et₂O (10 mL) was poured into the reaction mixture. The resulting precipitate was filtered, washed with an excess of Et₂O, and dried *in vacuo* to furnish carboxylic acid **13a** (14 mg, 11 μ mol, 72%) as a yellow foam.

1H -NMR (600 MHz, DMSO- d_6): $\delta = 12.37$ (s, 1 H, OH), 12.30 (s, 1 H, OH), 10.81 (s, 1 H, CONH), 10.63 (s, 1 H, CONH), 10.61 (s, 1 H, CONH), 10.58 (s, 1 H, CONH), 10.52 (s, 1 H, CONH), 9.45 (s, 1 H, CONH), 9.41 (s, 1 H, CONH), 8.47 (d, $J = 7.7$ Hz, 1 H, CONH), 8.40–8.38 (m, 2 H, Ar-H), 8.22–8.19 (m, 2 H, Ar-H), 8.05–8.04 (m, 2 H, Ar-H), 8.00–7.95 (m, 8 H, Ar-H), 7.91–7.89 (m, 6 H, Ar-H), 7.87–7.84 (m, 6 H, Ar-H), 7.73–7.71 (m, 2 H, Ar-H), 7.55 (bs, 1 H, CONH₂), 7.48 (bs, 1 H, CONH₂), 4.92 (t, $J = 7.8$ Hz, 1 H, CHNH), 4.58–4.53 (m, 2 H, CHMe₂), 4.09 (d, $J = 8.2$ Hz, 1 H, CHOMe), 3.31 (s, 3 H, OMe), 1.29–1.27 (m, 12 H, CHMe₂) ppm; ^{13}C -NMR (150 MHz, DMSO- d_6): $\delta = 170.9$ (q, CONH₂), 168.8 (q, C=O), 168.7 (q, C=O), 168.5 (q, C=O), 166.9 (q, C=O), 165.5 (q, C=O), 165.3 (q, C=O), 164.3 (q, C=O), 164.3 (q, C=O), 164.3 (q, C=O), 157.8 (q, quartet, $J = 33.9$ Hz, F₃CCO₂), 154.2 (q, COH), 154.1 (q, COH), 149.3 (Ar-C), 142.3 (Ar-C), 142.0 (Ar-C), 141.8 (Ar-C), 140.3 (Ar-C), 137.1 (Ar-C), 136.4 (Ar-C), 136.3 (Ar-C), 130.3 (Ar-C), 130.2 (Ar-C), 129.4 (Ar-C), 129.4 (Ar-C), 129.0 (Ar-C), 129.0 (Ar-C), 128.7 (Ar-C), 128.7 (Ar-C), 128.4 (Ar-C), 128.4 (Ar-C), 128.3 (Ar-C), 128.3 (Ar-C), 128.3 (Ar-C), 128.3 (Ar-C), 121.2 (q, quartet, $J = 515.2$ Hz, F₃CCO₂), 120.8 (Ar-C), 120.8 (Ar-C), 120.7 (Ar-C), 119.8 (Ar-C), 119.7 (Ar-C), 119.0 (Ar-C), 119.0 (Ar-C), 112.5 (Ar-C), 112.3 (Ar-C), 112.2 (Ar-C), 74.9 (t, CHMe₂), 74.9 (t, CHMe₂), 57.8 (p, OMe), 55.8 (t, CHNH), 22.3 (p, CHMe₂), 22.3 (p, CHMe₂) ppm; HRMS (ESI): m/z calculated for C₆₇H₅₉N₁₀O₁₈ [M-H]⁻: 1291.4009; found: 1291.4042; $[\alpha]_D^{28} = +14.0^\circ$ (c 0.1, DMSO- d_6); R_f (10% MeOH/ CH_2Cl_2): 0.32.

Conformational analyses

The 1H , ^{13}C , HSQC, HMBC and NOESY spectra recorded in DMSO- d_6 were used for assignment and were recorded on a 500 MHz Bruker Avance NEO spectrometer equipped with a 5 mm TXO cryogenic probe for **12b**, and on a 600 MHz Bruker Avance NEO spectrometer equipped with a 5 mm TCI cryogenic probe for **13b** and **13c**.

The 3D conformations of cystobactamids **13c** and **13b** were computationally sampled by Monte Carlo systematic torsional sampling (MCSTS), using 500 000 Monte Carlo steps, with 72 steps per rotatable bond, the OPLS4 force-field and an 0.5 Å RMSD cut-off. The ensembles were further sized down by removal of redundant conformers with a 2.0 Å RMSD cut-off for **13b**, giving rise to a total of 390 conformations, and an RMSD cut-off of 1.0 Å for **13c**, resulting in 195 conformations. For the RDC analysis of **13c**, a redundant conformer elimination with a 1.5 Å cut-off was performed, giving rise to an ensemble of 35 conformations. This smaller ensemble for RDC analysis was selected, because the software MSpin can handle smaller input ensembles better.

NOESY spectra of the cystobactamids in DMSO-*d*₆ were recorded on a 500 or a 600 MHz Bruker Avance NEO spectrometer. The spectra were recorded with 16 transients, a d1 relaxation delay of 2.5 s, 2048 points in the direct dimension, 512 increments and 700 ms mixing time at 25 °C.

Cross-peak intensities were extracted through integration and normalized $I_{ab} = ((\text{cross-peak}_{ab} \times \text{cross-peak}_{ba}) / (\text{diagonal-peak}_a \times \text{diagonal-peak}_b))^{(1/2)}$ for protons H_a and H_b. The interproton distances were estimated for 51 correlations of **13b** and 47 correlations of **13c** according to $r_{ab} = r_{ref}(I_{ref}/I_{ab})^{(1/6)}$, where r_{ab} is the distance between protons H_a and H_b in Ångströms, r_{ref} is 2.43 Å (ortho proton at position 1–6 or 3–4), and I_{ref} and I_{ab} are the normalized intensities of the respective proton-pairs. Tables S5 and S6 of the supporting information show all NOE correlations that were found for **13b** and **13c**, respectively.

Two sets of f2-coupled perfect-clip HSQC spectra were recorded; one under isotropic and one under anisotropic conditions. The spectra were recorded on a 10.2 mM solution of **13c**. For the anisotropic spectra, the sample in DMSO-*d*₆ was used to hydrate the PAN gel inside an NewEra compression NMR tube. The gel was swollen for at least 16 h before running the anisotropic NMR experiments. All spectra were recorded on a 600 MHz Bruker Avance NEO equipped with a 5 mm TCI cryogenic probe at 25 °C. HSQC spectra, coupled along the f2 dimension, were recorded with 32 transients, 512 increments, 4096 points in f2 and a relaxation delay of 1 s. The obtained RDC's for **13c** are summarized in Table S11 of the Supporting information. RDC analysis of **13c** was performed with the software MSpin 2.6.0.

Biological Activity

Minimal inhibitory concentrations (MIC). MIC values were determined in standard microbroth dilution assays as described elsewhere.^[1,2]

Microscale Thermophoresis (MST) experiments

DNA gyrase from Escherichia coli (D0690, Sigma-Aldrich) was dialyzed against 100 mM sodium bicarbonate buffer pH 8.5 at 4 °C for 16 h. The protein was labeled using the EZLabel Protein FITC Labeling Kit (ab288089, abcam) following the manufacturer's instructions. Cystobactamid (CN-861-2) was dissolved at 20 mM in DMSO, and seven 1:5 dilutions were prepared in DMSO. Each final MST sample contained 50 nM FITC-Gyrase and CN-861-2 in concentrations ranging from 500 μM to 6.4 nM, yielding a final DMSO concentration of 2.5%. FITC-DNA primer and unlabeled primer for AT primer pairs: 5'-[CY5]-ATTAATTTTATTTAATTTAAATA-TTTAAAT-3' and AT 5'-ATTTAAATTTTAAATTTAAATAATTTAAT-3' and Cy5-GC primer pairs: 5'-[CY5]-GCCGGTGC GCGGCCA-CCGGTCCGCGCAGGC-3' and GC 5'-GCCTCGCGC GACCGG-TGGCCGCGCACC GGC-3'. The MST measurement was performed

using a NanoTemper Monolith NT.115 G008, 20% excitation power and 40% MST power.

Supporting Information

The authors have cited additional references within the Supporting Information (Ref. [32–34]).

Acknowledgements

This work was supported by the German Center for Infection Research (DZIF) and the Bundesministerium für Bildung und Forschung (BMBF; project OpCyBac 16GW0220). We thank Armando Navarro-Vazquez (Universidade Federal de Pernambuco, Brazil) for helpful discussions and a generous donation of PAN gel for alignment. We also thank Viktoria George and Alexandra Amann for technical assistance with cell-based activity screening. This study made use of the NMR Uppsala infrastructure, which is funded by the Department of Chemistry – BMC and the Disciplinary Domain of Medicine and Pharmacy. The computations were enabled by resources provided by the Swedish National Infrastructure for Computing (SNIC) at Tetralith, partially funded by the Swedish Research Council through grant agreement no. 2018-05973, under project numbers 2021/5-359 and 2021/22-350. We are grateful to the Swedish Research Council for financial support (2020-03431). M. E. and A. K. thank the Wenner-Gren Foundation for financial support (GFOh2022-0018). Open Access funding enabled and organized by Projekt DEAL.

Conflict of Interests

The authors declare no conflict of interests.

Data Availability Statement

The data that support the findings of this study are available in the supplementary material of this article.

Keywords: antibiotics · cystobactamids · DNA-binding · NMR-studies · oligoamides

- [1] A. Kluczyk, T. Popek, T. Kiyota, P. De Macedo, P. Stefanowicz, C. Lazar, Y. Konishi, *Curr. Med. Chem.* **2002**, *9*, 1871–1992.
- [2] Review: R. Gopalakrishnan, A. I. Frolov, L. Knerr, W. J. Drury III, E. Valeur, *J. Med. Chem.* **2016**, *59*, 9599–9621.
- [3] a) V. Azzarito, K. Long, N. S. Murphy, A. J. Wilson, *Nat. Chem.* **2013**, *5*, 161–173; b) A. S. Ripka, D. H. Rich, *Curr. Opin. Chem. Biol.* **1998**, *2*, 441–452; c) I. Arrata, C. M. Grison, H. M. Coubrough, P. Prabhakaran, M. A. Little, D. C. Tomlinson, M. E. Webb, A. J. Wilson, *Org. Biomol. Chem.* **2019**, *17*, 3861–3867.
- [4] a) T. Edwards, A. Wilson, *Amino Acids* **2011**, *41*, 743–754; b) B. N. Bullock, A. L. Jochim, P. S. Arora, *J. Am. Chem. Soc.* **2011**, *133*, 14220–14223.
- [5] Review: R. Gopalakrishnan, A. I. Frolov, L. Knerr, W. J. Drury, III, E. Valeur, *J. Med. Chem.* **2016**, *59*, 9599–9621.

- [6] a) V. Azzarito, K. Long, N. S. Murphy, A. J. Wilson, *Nat. Chem.* **2013**, *5*, 161–173; b) A. S. Ripka, D. H. Rich, *Curr. Opin. Chem. Biol.* **1998**, *2*, 441–452; c) Y. Hamuro, S. J. Geib, A. D. Hamilton, *Angew. Chem. Int. Ed. Engl.* **1994**, *33*, 446–448.
- [7] T. Edwards, A. Wilson, *Amino Acids* **2011**, *41*, 743–754.
- [8] J. L. Yap, X. Cao, K. Vanommeslaeghe, K.-Y. Jung, C. Peddaboina, P. T. Wilder, A. Nan, A. D. Mackerell, Jr, W. R. Smythe, S. Fletcher, *Org. Biomol. Chem.* **2012**, *10*, 2928–2933.
- [9] a) S. Kumar, A. D. Hamilton, *J. Am. Chem. Soc.* **2017**, *139*, 5744–5755; b) S. Kumar, A. H. Henning-Knechtel, M. Magzoub, A. D. Hamilton, *J. Am. Chem. Soc.* **2018**, *140*, 6562–6574.
- [10] S. Kumar, A. Henning-Knechtel, I. Chehade, M. Magzoub, A. D. Hamilton, *J. Am. Chem. Soc.* **2017**, *139*, 17098–17108.
- [11] C.-H. Lee, J.-R. Yu, S. Kumar, Y. Jin, G. LeRoy, N. Bhanu, S. Kaneko, B. A. Garcia, A. D. Hamilton, D. Reinberg, *Mol. Cell* **2018**, *70*, 422–434.
- [12] D. Maity, S. Kumar, F. Curreli, A. K. Debnath, A. D. Hamilton, *Chem. Eur. J.* **2019**, *25*, 7265–7269.
- [13] a) K. Ziach, C. Chollet, V. Parissi, P. Prabhakaran, M. Marchivie, V. Corvaglia, P. P. Bose, K. Laxmi-Reddy, F. Godde, J.-M. Schmitter, S. Chaignepain, P. Pourquier, I. Huc, *Nat. Chem.* **2018**, *10*, 511–518; b) V. Corvaglia, D. Carbajo, P. Prabhakaran, K. Ziach, P. K. Mandal, V. Dos Santos, C. Legeay, R. Vogel, V. Parissi, P. Pourquier, I. Huc, *Nucl. Acids Res.* **2019**, *47*, 5511–5521.
- [14] a) P. B. Dervan, M. M. Becker, *J. Am. Chem. Soc.* **1978**, *100*, 1968–1970; b) M. M. Becker, P. B. Dervan, *J. Am. Chem. Soc.* **1979**, *101*, 3664–3666; c) P. B. Dervan, *Isr. J. Chem.* **2019**, *59*, 71–83.
- [15] T. Seedorf, A. Kirschning, D. Solga, *Chem. Eur. J.* **2021**, *27*, 7321–7329.
- [16] S. Baumann, J. Herrmann, R. Raju, H. Steinmetz, K. I. Mohr, S. Hüttel, K. Harmrolfs, M. Stadler, R. Müller, *Angew. Chem. Int. Ed. Engl.* **2014**, *53*, 14605–14609.
- [17] S. Hüttel, G. Testolin, J. Herrmann, T. Planke, F. Gille, M. Moreno, M. Stadler, M. Brönstrup, A. Kirschning, R. Müller, *Angew. Chem. Int. Ed.* **2017**, *56*, 12760–12764.
- [18] a) B. Cheng, R. Müller, D. Trauner, *Angew. Chem. Int. Ed.* **2017**, *56*, 12755–12759; b) T. Planke, M. Moreno, J. Fohrer, F. Gille, A. Kanakis, M. D. Norris, M. Siebke, L. L. Wang, S. Hüttel, R. Müller, A. Kirschning, *Org. Lett.* **2019**, *21*, 1359–1363.
- [19] a) M. Moreno, W. A. M. Elgaher, J. Herrmann, N. Schläger, M. M. Hamed, S. Baumann, R. Müller, R. W. Hartmann, A. Kirschning, *Synlett* **2015**, *26*, 1175–1178; b) M. Moeller, M. D. Norris, T. Planke, K. Cirnski, J. Herrmann, R. Müller, A. Kirschning, *Org. Lett.* **2019**, *21*, 8369–8372; c) T. Planke, K. Cirnski, J. Herrmann, R. Müller, A. Kirschning, *Chem. Eur. J.* **2020**, *26*, 4289–4296; d) G. Testolin, K. Cirnski, K. Rox, H. Prochnow, V. Fetz, C. Grandclaudon, T. Mollner, A. Baiyoumy, A. Ritter, C. Leitner, J. Krull, H. A. van den Vassort, S. Sordello, M. M. Hamed, W. A. M. Elgaher, J. Herrmann, R. W. Hartmann, R. Müller, M. Brönstrup, *Chem. Sci.* **2020**, *11*, 1316–1334; e) W. A. M. Elgaher, M. M. Hamed, S. Baumann, J. Herrmann, L. Siebenbürger, J. Krull, K. Cirnski, A. Kirschning, M. Brönstrup, R. Müller, R. W. Hartmann, *Chem. Eur. J.* **2020**, *26*, 7219–7225.
- [20] Y. Kim, H. J. Kim, G. W. Kim, K. Cho, S. Takahashi, H. Koshino, W. G. Kim, *J. Nat. Prod.* **2016**, *79*, 2223.
- [21] a) S. Cociancich, D. Pesic, D. Petras, S. Uhlmann, J. Kretz, V. Schubert, L. Vieweg, S. Duplan, M. Marguerettaz, J. Noell, I. Pieretti, M. Hügelland, S. Kemper, A. Mainz, P. Rott, M. Royer, R. D. Süßmuth, *Nat. Chem. Biol.* **2015**, *11*, 195–197; b) L. Kleebauer, L. Zborovsky, K. Hommernick, M. Seidel, J. B. Weston, R. D. Süßmuth, *Org. Lett.* **2021**, *23*, 7023–7027; c) L. Zborovsky, L. Kleebauer, M. Seidel, A. Kostenko, L. v. Eckardstein, G. O. Gombert, J. B. Weston, R. D. Süßmuth, *Chem. Sci.* **2021**, *12*, 14606–14617.
- [22] E. Michalczyk, K. Hommernick, I. Behroz, M. Kulike, Z. Pakosz-Stępień, L. Mazurek, M. Seidel, M. Kunert, K. Santos, H. von Moeller, B. Loll, J. B. Weston, A. Mainz, J. G. Hedde, R. D. Süßmuth, D. Ghilarov, *Nat. Catal.* **2023**, *6*, 52–67.
- [23] a) S. A. Aldossary, *Biomed. Pharmacol. J.* **2019**, *12*, 7–15; b) A. C. Finlay, F. A. Hochstein, B. A. Sobin, F. X. Murphy, *J. Am. Chem. Soc.* **1951**, *73*, 341–343; c) F. Arcamone, S. Penco, P. Orezzi, V. Nicoletta, A. Pirelli, *Nature* **1964**, *203*, 1064–1065.
- [24] a) Y. Becker, *Monogr. Virol.* **1976**, *11*, 1–130; b) C. E. Hoffmann, *Ann. Rep. Med. Chem.* (Ed.: M. Gordon), Academic Press, New York, **1976**, *Vol. 11*, pp. 128–137; c) J. W. Corcoran, F. E. Hahn, J. F. Snell, K. L. Arora, in *Mechanism of Action of Antimicrobial and Antitumor Agents*; Springer Berlin Heidelberg, Berlin, Heidelberg, **1975**.
- [25] a) M. Mrksich, P. B. Dervan, *J. Am. Chem. Soc.* **1993**, *115*, 9892–9899; b) M. Mrksich, P. B. Dervan, *J. Am. Chem. Soc.* **1994**, *116*, 3663–3664.
- [26] C. P. Butts, C. R. Jones, E. C. Towers, J. L. Flynn, L. Appleby, N. J. Barron, *Org. Biomol. Chem.* **2011**, *9*, 177–184.
- [27] Y. Z. Liu, A. Navarro-Vazquez, R. R. Gil, C. Griesinger, G. E. Martin, R. T. Williamson, *Nat. Protoc.* **2019**, *14*, 217–247.
- [28] C. M. Thiele, *Eur. J. Org. Chem.* **2008**, 5673–5685.
- [29] A. Navarro-Vázquez, *Magn. Reson. Chem.* **2012**, *50*, S73–S79.
- [30] G. Cornilescu, J. L. Marquardt, M. Ottiger, A. Bax, *J. Am. Chem. Soc.* **1998**, *120*, 6836–6837.
- [31] a) V. Guelev, S. Sorey, D. W. Hoffman, B. L. Iverson, *J. Am. Chem. Soc.* **2002**, *124*, 2864–2865; b) C. L. Brown, M. M. Harding, *J. Mol. Recognit.* **1994**, *7*, 215–220.

Manuscript received: November 15, 2023
Accepted manuscript online: January 13, 2024
Version of record online: February 15, 2024